

CHAPTER

12

Discrete Fourier transform

In Chapter 11, we introduced the discrete-time Fourier transform (DTFT) that provides us with alternative representations for DT sequences. The DTFT transforms a DT sequence $x[k]$ into a function $X(\Omega)$ in the DTFT frequency domain Ω . The independent variable Ω is continuous and is confined to the range $-\pi \leq \Omega < \pi$. With the increased use of digital computers and specialized hardware in signal processing, interest has focused around transforms that are suitable for digital computations. Because of the continuous nature of Ω , direct implementation of the DTFT is not suitable on such digital devices. This chapter introduces the discrete Fourier transform (DFT), which can be computed efficiently on digital computers and other digital signal processing (DSP) boards.

The DFT is an extension of the DTFT for time-limited sequences with an additional restriction that the frequency Ω is discretized to a finite set of values given by $\Omega = 2\pi r/M$, for $0 \leq r \leq (M - 1)$. The number M of the frequency samples can have any value, but is typically set equal to the length N of the time-limited sequence $x[k]$. If M is chosen to be a power of 2, then it is possible to derive extremely efficient implementations of the DFT. These implementations are collectively referred to as the fast Fourier transform (FFT) and, for an M -point DFT, have a computational complexity of $O(M \log_2 M)$. This chapter discusses a popular FFT implementation and extends the theoretical DTFT results derived in Chapter 11 to the DFT.

The organization of this chapter is as follows. Section 12.1 motivates the discussion of the DFT by expressing it as a special case of the continuous-time Fourier transform (CTFT). The formal definition of the DFT is presented in Section 12.2, including its matrix-vector representation. Section 12.3 applies the DFT to estimation of the spectra of both DT and CT signals. Section 12.4 derives important properties of the DFT, while Section 12.5 uses the DFT as a tool to convolve two DT sequences in the frequency domain. A fast implementation of the DFT based on the decimation-in-time algorithm is presented in Section 12.6. Finally, Section 12.7 concludes the chapter with a summary of the important concepts.

12.1 Continuous to discrete Fourier transform

In order to motivate the discussion of the DFT, let us assume that we are interested in computing the CTFT of a CT signal $x(t)$ using a digital computer. The three main steps involved in the computation of the CTFT are illustrated in Fig. 12.1. The waveforms for the CT signal $x(t)$ and its CTFT $X(\omega)$, shown in Figs 12.1(a) and (b), are arbitrarily chosen, so the following procedure applies to any CT signal. A brief explanation of each of the three steps is provided below.

Step 1: Analog-to-digital conversion In order to store a CT signal into a digital computer, the CT signal is digitized. This is achieved through two processes known as sampling and quantization, collectively referred to as analog-to-digital (A/D) conversion by convention. In this discussion, we only consider sampling, ignoring the distortion introduced by quantization. The CT signal $x(t)$ is sampled by multiplying it by an impulse train:

$$s_1(t) = \sum_{m=-\infty}^{\infty} \delta(t - mT_1), \quad (12.1)$$

illustrated in Fig. 12.1(c). The sampled waveform is given by $x_1(t) = x(t)s_1(t)$, which is shown in Fig. 12.1(e). Since multiplication in the time domain is equivalent to convolution in the frequency domain, the CTFT $X_1(\omega)$ of the sampled signal $x_1(t)$ is given by the following transform pair:

$$\begin{aligned} x_1(t) = x(t) \times \sum_{m=-\infty}^{\infty} \delta(t - mT_1) &\stackrel{\text{CTFT}}{\longleftrightarrow} X_1(\omega) \\ &= \frac{1}{2\pi} \left[X(\omega) * \frac{2\pi}{T_1} \sum_{m=-\infty}^{\infty} \delta\left(\omega - \frac{2m\pi}{T_1}\right) \right] \end{aligned} \quad (12.2)$$

or

$$x_1(t) = \sum_{m=-\infty}^{\infty} x(mT_1)\delta(t - mT_1) \stackrel{\text{CTFT}}{\longleftrightarrow} X_1(\omega) = \frac{1}{T_1} \sum_{m=-\infty}^{\infty} X\left(\omega - \frac{2m\pi}{T_1}\right). \quad (12.3)$$

The above result is derived in Eq. (9.5) of Chapter 9 and is graphically illustrated in Figs 12.1(b), (d), and (f), where we note that the spacing between adjacent replicas of $X(\omega)$ in $X_1(\omega)$ is given by $2\pi/T_1$. Since no restriction is imposed on the bandwidth of the CT signal $x(t)$, limited aliasing may also be introduced in $X_1(\omega)$.

To derive the discretized representation of $x(t)$ from Eq. (12.3), sampling is followed by an additional step (shown in Fig. 12.1(g)), where the CT impulses are converted to the DT impulses. Equation (12.3) can now be extended to

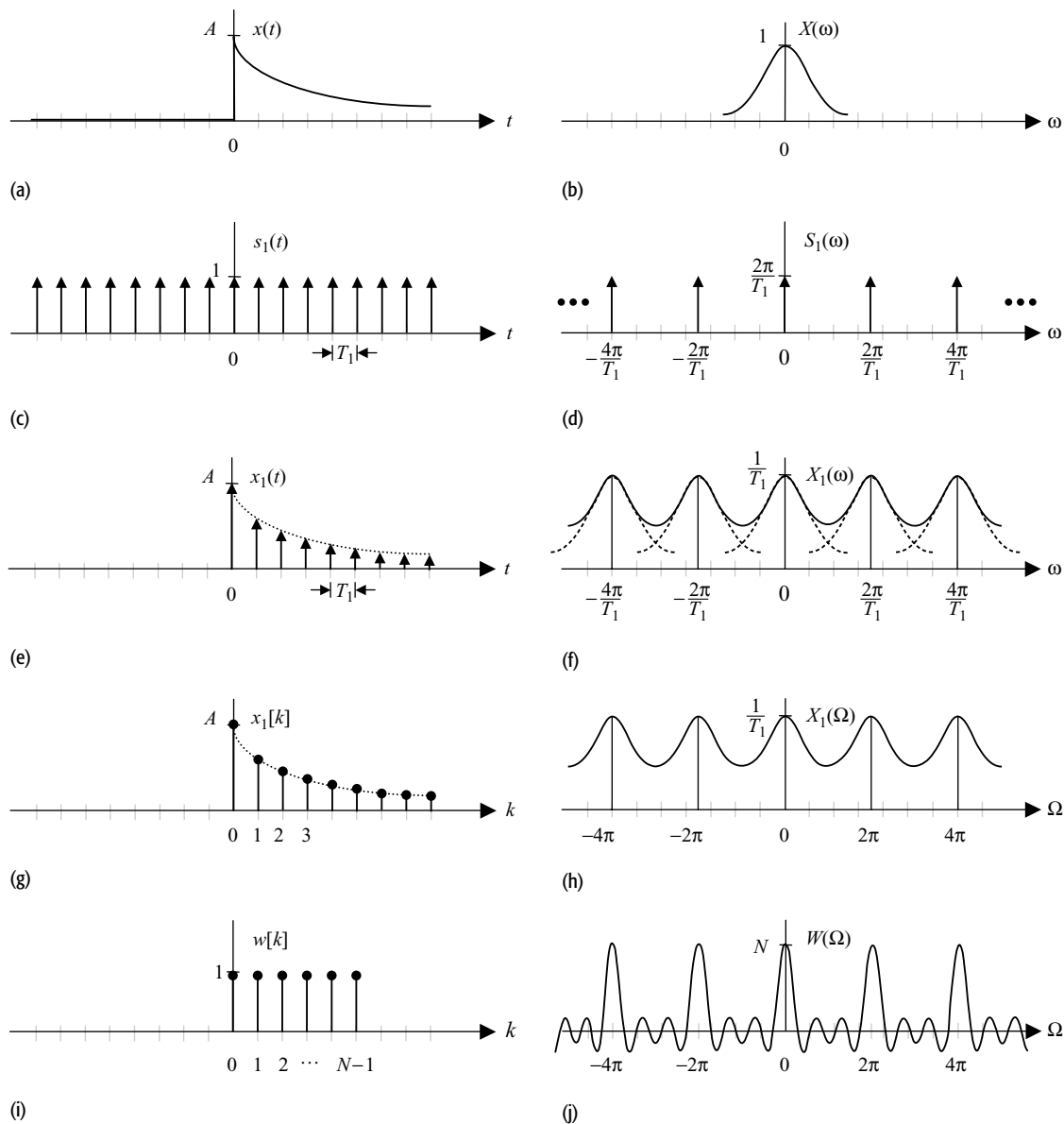


Fig. 12.1. Graphical derivation of the discrete Fourier transform pair. Original CT signal. (b) CTFT of the original CT signal. (c) Impulse train sampling of CT signal. (d) CTFT of the impulse train in part (c). (e) CT sampled signal. (f) CTFT of the sampled signal in part (e). (g) DT representation of CT signal in part (a). (h) DTFT of the DT representation in part (g). (i) Rectangular windowing sequence. (j) DTFT of the rectangular window. (k) Time-limited sequence representing part (g). (l) DTFT of time-limited sequence in part (k). (m) Inverse DTFT of frequency-domain impulse train in part (n). (n) Frequency-domain impulse train.

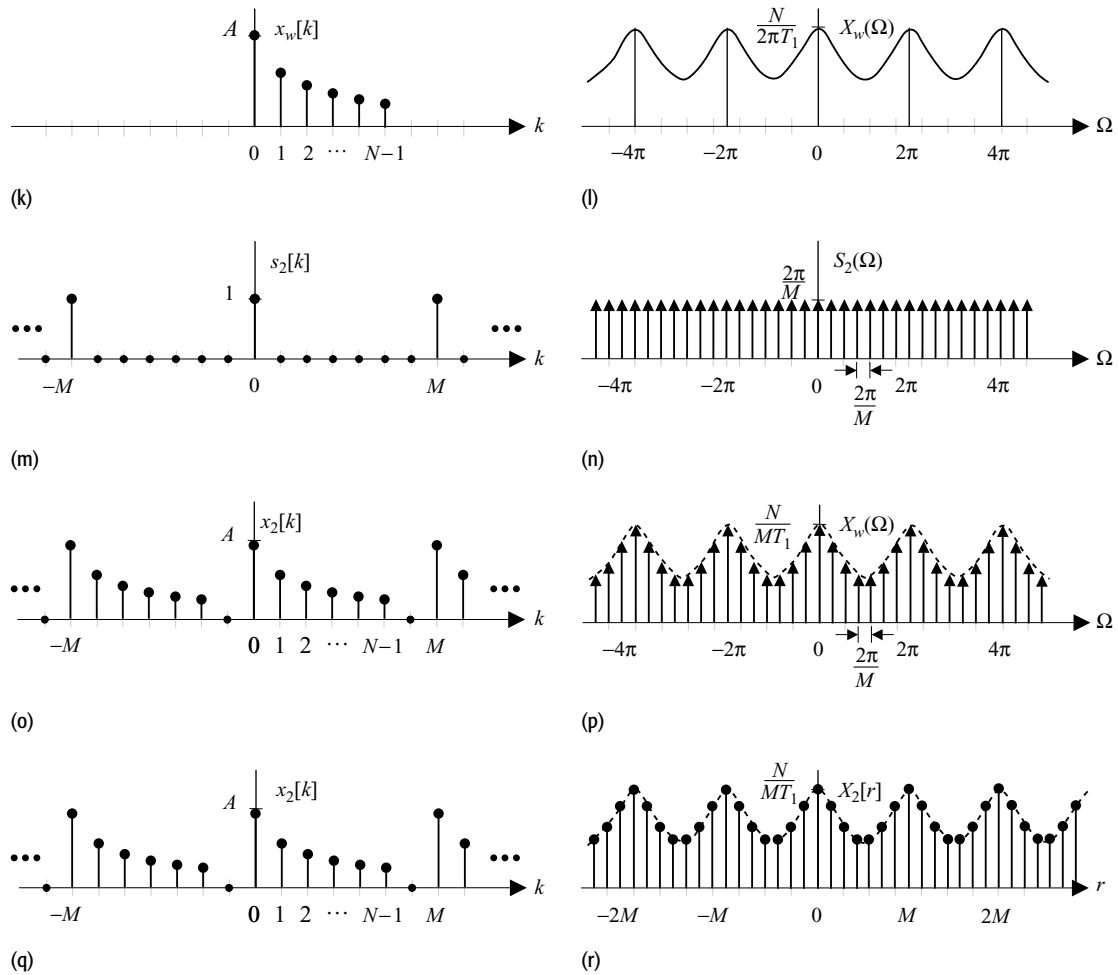


Fig. 12.1. (cont.)

derive the DTFT of the DT sequence $x_1[k]$ as follows:

$$x_1[k] = \sum_{m=-\infty}^{\infty} x(mT_1)\delta(t - mT_1). \quad (12.4)$$

Taking the DTFT of both sides of Eq. (12.4) yields

$$X_1(\omega) = \sum_{m=-\infty}^{\infty} x(mT_1)e^{-j\omega mT_1}. \quad (12.5)$$

Substituting $x_1[m] = x(mT_1)$ and $\Omega = \omega T_1$ in Eq. (12.5) leads to

$$X_1(\Omega) = X_1(\omega)|_{\omega=\Omega/T_1} = \sum_{m=-\infty}^{\infty} x_1[m]e^{-jm\Omega},$$

12 Discrete Fourier transform

which is the standard definition of the DTFT introduced in Chapter 11. The DTFT spectrum $X_1(\Omega)$ of $x_1[k]$ is obtained by changing the frequency axis ω of the CTFT spectrum $X_1(\omega)$ according to the relationship $\Omega = \omega T_1$. The DTFT spectrum $X_1(\Omega)$ is illustrated in Fig. 12.1(h).

Step 2: Time limitation The discretized signal $x_1[k]$ can possibly be of infinite length. Therefore, it is important to truncate the length of the discretized signal $x_1[k]$ to a finite number of samples. This is achieved by multiplying the discretized signal by a rectangular window,

$$w[k] = \begin{cases} 1 & 0 \leq k \leq (N - 1) \\ 0 & \text{elsewhere,} \end{cases} \quad (12.6)$$

of length N . The DTFT $X_w(\Omega)$ of the time-limited signal $x_w[k] = x_1[k]w[k]$ is obtained by convolving the DTFT $X_1(\Omega)$ with the DTFT $W(\Omega)$ of the rectangular window, which is a sinc function. In terms of $X_1(\Omega)$, the DTFT $X_w(\Omega)$ of the time-limited signal is given by

$$X_w(\Omega) = \frac{1}{2\pi} \left[X_1(\Omega) \otimes \frac{\sin(0.5N\Omega)}{\sin(0.5\Omega)} e^{-j(N-1)\Omega/2} \right], \quad (12.7)$$

which is shown in Fig. 12.1(i) with its time-limited representation $x_w[k]$ plotted in Fig. 12.1(k). Symbol \otimes in Eq. (12.7) denotes the circular convolution.

Step 3: Frequency sampling The DTFT $X_w(\Omega)$ of the time-limited signal $x_w[k]$ is a continuous function of Ω and must be discretized to be stored on the digital computer. This is achieved by multiplying $X_w(\Omega)$ by a frequency-domain impulse train, whose DTFT is given by

$$S_2(\Omega) = \frac{2\pi}{M} \sum_{m=-\infty}^{\infty} \delta\left(\Omega - \frac{2\pi m}{M}\right). \quad (12.8)$$

The discretized version of the DTFT $X_w(\Omega)$ is therefore expressed as follows:

$$\begin{aligned} X_2(\Omega) = X_w(\Omega)S_2(\Omega) &= \frac{1}{M} \left[X_1(\Omega) \otimes \frac{\sin(0.5N\Omega)}{\sin(0.5\Omega)} e^{-j(N-1)\Omega/2} \right] \\ &\times \sum_{m=-\infty}^{\infty} \delta\left(\Omega - \frac{2\pi m}{M}\right). \end{aligned} \quad (12.9)$$

The DTFT $X_2(\Omega)$ is shown in Fig. 12.1(p), where the number M of frequency samples within one period ($-\pi \leq \Omega \leq \pi$) of $X_2(\Omega)$ depends upon the fundamental frequency $\Omega_2 = 2\pi/M$ of the impulse train $S_2(\Omega)$. Taking the inverse DTFT of Eq. (12.9), the time-domain representation $x_2[k]$ of the frequency-sampled signal $X_2(\Omega)$ is given by

$$x_2[k] = [x_w[k] * s_2[k]] = [x_1[k] \cdot w[k]] * \sum_{m=-\infty}^{\infty} \delta(k - mM), \quad (12.10)$$

and is shown in Fig. 12.1(o).

The discretized version of the DTFT $X_w(\Omega)$ is referred to as the discrete Fourier transform (DFT) and is generally represented as a function of the frequency index r corresponding to DTFT frequency $\Omega_r = 2r\pi/M$, for $0 \leq r \leq (M-1)$. To derive the expression for the DFT, we substitute $\Omega = 2r\pi/M$ in the following definition of the DTFT:

$$X_2(\Omega) = \sum_{k=0}^{N-1} x_2[k]e^{-jk\Omega}, \quad (12.11)$$

where we have assumed $x_2[k]$ to be a time-limited sequence of length N . Equation (12.11) reduces as follows:

$$X_2(\Omega_r) = \sum_{k=0}^{N-1} x_2[k]e^{-j(2\pi kr/M)}, \quad (12.12)$$

for $0 \leq r \leq (M-1)$. Equation (12.12) defines the discrete Fourier transform (DFT) and can easily be implemented on a digital device since it converts a discrete number N of input samples in $x_2[k]$ to a discrete number M of DFT samples in $X_2(\Omega_r)$. To illustrate the discrete nature of the DFT, the DFT $X_2(\Omega_r)$ is also denoted as $X_2[r]$. The DFT spectrum $X_2[r]$ is plotted in Fig. 12.1(r).

Let us now return to the original problem of determining the CTFT $X(\omega)$ of the original CT signal $x(t)$ on a digital device. Given $X_2[r] = X_2(\Omega_r)$, it is straightforward to derive the CTFT $X(\omega)$ of the original CT signal $x(t)$ by comparing the CTFT spectrum, shown in Fig. 12.1(b), with the DFT spectrum, shown in Fig. 12.1(r). We note that one period of the DFT spectrum within the range $-0.5(M-1) \leq r \leq 0.5(M-1)$ (assuming M to be odd) is a fairly good approximation of the CTFT spectrum. This observation leads to the following relationship:

$$X(\omega_r) \approx \frac{MT_1}{N} X_2[r] = \frac{MT_1}{N} \sum_{k=0}^{N-1} x_2[k]e^{-j(2\pi kr/M)}, \quad (12.13)$$

where the CT frequencies $\omega_r = \Omega_r/T_1 = 2\pi r/(M \times T_1)$ for $-0.5(M-1) \leq r \leq 0.5(M-1)$.

Although Fig. 12.1 illustrates the validity of Eq. (12.1) by showing that the CTFT $X(\omega)$ and the DFT $X_2[r]$ are similar, there are slight variations in the two spectra. These variations result from aliasing in Step 1 and loss of samples in Step 2. If the CT signal $x(t)$ is sampled at a sampling rate less than the Nyquist limit, aliasing between adjacent replicas distorts the signal. A second distortion is introduced when the sampled sequence $x_1[k]$ is multiplied by the rectangular window $w[k]$ to limit its length to N samples. Some samples of $x_1[k]$ are lost in the process. To eliminate aliasing, the CT signal $x(t)$ should be band-limited, whereas elimination of the time-limited distortion requires $x(t)$ to be of finite length. These are contradictory requirements since a CT signal cannot be both time-limited and band-limited at the same time. As a result, at least one of the

aforementioned distortions would always be present when approximating the CTFT with the DFT. This implies that Eq. (12.12) is an approximation for the CTFT $X(\omega)$ that, even at its best, only leads to a near-optimal estimation of the spectral content of the CT signal.

On the other hand, the DFT representation provides an accurate estimate of the DTFT of a time-limited sequence $x[k]$ of length N . By comparing the DFT spectrum, Fig. 12.1(h), with the DFT spectrum, Fig. 12.1(r), the relationship between the DTFT $X_2(\Omega)$ and the DFT $X_2[r]$ is derived. Except for a factor of K/M , we note that $X_2[r]$ provides samples of the DTFT at discrete frequencies $\Omega_r = 2\pi r/M$, for $0 \leq r \leq (M-1)$. The relationship between the DTFT and DFT is therefore given by

$$X_2(\Omega_r) = \frac{N}{M} X_2[r] = \frac{N}{M} \sum_{k=0}^{N-1} x_2[k] e^{-j(2\pi kr/M)} \quad (12.14)$$

for $\Omega_r = 2\pi r/M$, for $0 \leq r \leq (M-1)$. We now proceed with the formal definitions for the DFT.

12.2 Discrete Fourier transform

Based on our discussion in Section 12.1, the M -point DFT and inverse DFT for a time-limited sequence $x[k]$, which is non-zero within the limits $0 \leq k \leq (N-1)$, is given by

$$\text{DFT synthesis equation} \quad x[k] = \frac{1}{M} \sum_{r=0}^{M-1} X[r] e^{j(2\pi kr/M)} \quad \text{for } 0 \leq k \leq (N-1); \quad (12.15)$$

$$\text{DFT analysis equation} \quad X[r] = \sum_{k=0}^{N-1} x[k] e^{-j(2\pi kr/M)} \quad \text{for } 0 \leq r \leq (M-1). \quad (12.16)$$

Equation (12.16) was derived in Section 12.1. By substituting the expression for $x[k]$ from the synthesis equation, Eq. (12.15), the analysis equation, Eq. (12.16), can be formally proved. The formal proofs of the DFT pair are left as an exercise for the reader in Problem 12.1. In Eqs (12.15) and (12.16), the length M of the DFT is typically set to be greater or equal to the length N of the aperiodic sequence $x[k]$. Unless otherwise stated, we assume $M = N$ in the discussion that follows. Collectively, the DFT pair is denoted as

$$x[k] \xleftrightarrow{\text{DFT}} X[r]. \quad (12.17)$$

Examples 12.1 and 12.2 illustrate the steps involved in calculating the DFTs of aperiodic sequences.

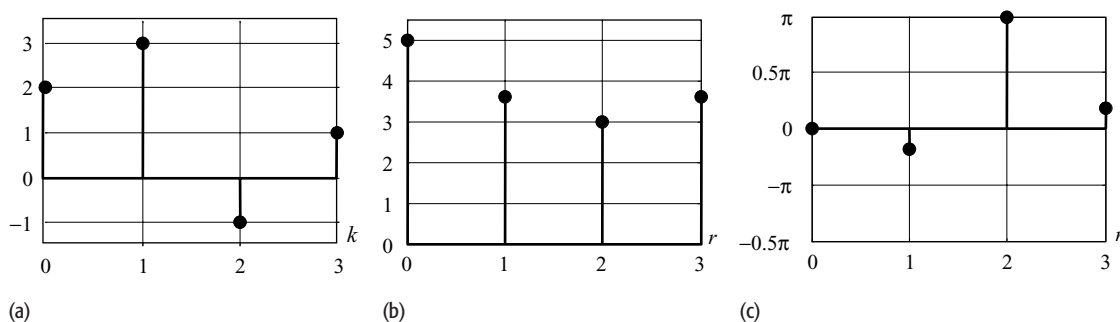


Fig. 12.2. (a) DT sequence $x[k]$; (b) magnitude spectrum and (c) phase spectrum of its DTFT $X[r]$ computed in Example 12.1.

Example 12.1

Calculate the four-point DFT of the aperiodic sequence $x[k]$ of length $N = 4$, which is defined as follows:

$$x[k] = \begin{cases} 2 & k = 0 \\ 3 & k = 1 \\ -1 & k = 2 \\ 1 & k = 3. \end{cases}$$

Solution

Using Eq. (12.14), the four-point DFT of $x[k]$ is given by

$$\begin{aligned} X[r] &= \sum_{k=0}^3 x[k]e^{-j(2\pi kr/4)} \\ &= 2 + 3 \times e^{-j(2\pi r/4)} - 1 \times e^{-j(2\pi(2)r/4)} + 1 \times e^{-j(2\pi(3)r/4)}, \end{aligned}$$

for $0 \leq r \leq 3$. On substituting different values of r , we obtain

$$r = 0 \quad X[0] = 2 + 3 - 1 + 1 = 5;$$

$$\begin{aligned} r = 1 \quad X[1] &= 2 + 3 \times e^{-j(2\pi/4)} - 1 \times e^{-j(2\pi(2)/4)} + 1 \times e^{-j(2\pi(3)/4)} \\ &= 2 + 3(-j) - 1(-1) + 1(j) = 3 - 2j; \end{aligned}$$

$$\begin{aligned} r = 2 \quad X[2] &= 2 + 3 \times e^{-j(2\pi(2)/4)} - 1 \times e^{-j(2\pi(2)(2)/4)} + 1 \times e^{-j(2\pi(3)(2)/4)} \\ &= 2 + 3(-1) - 1(1) + 1(-1) = -3; \end{aligned}$$

$$\begin{aligned} r = 3 \quad X[3] &= 2 + 3 \times e^{-j(2\pi(3)/4)} - 1 \times e^{-j(2\pi(2)(3)/4)} + 1 \times e^{-j(2\pi(3)(3)/4)} \\ &= 2 + 3(j) - 1(-1) + 1(-j) = 3 + j2. \end{aligned}$$

The magnitude and phase spectra of the DFT are plotted in Figs 12.2(b) and (c), respectively.

12 Discrete Fourier transform

Example 12.2

Calculate the inverse DFT of

$$X[r] = \begin{cases} 5 & r = 0 \\ 3 - j2 & r = 1 \\ -3 & r = 2 \\ 3 + j2 & r = 3. \end{cases}$$

Solution

Using Eq. (12.13), the inverse DFT of $X[r]$ is given by

$$x[k] = \frac{1}{4} \sum_{r=0}^3 X[r] e^{j(2\pi kr/4)} = \frac{1}{4} [5 + (3 - j2) \times e^{j(2\pi k/4)} - 3 \times e^{j(2\pi(2)k/4)} + (3 + j2) \times e^{j(2\pi(3)k/4)}],$$

for $0 \leq k \leq 3$. On substituting different values of k , we obtain

$$x[0] = \frac{1}{4} [5 + (3 - j2) - 3 + (3 + j2)] = 2;$$

$$\begin{aligned} x[1] &= \frac{1}{4} [5 + (3 - j2)e^{j(2\pi/4)} - 3e^{j(2\pi(2)/4)} + (3 + j2)e^{j(2\pi(3)/4)}] \\ &= \frac{1}{4} [5 + (3 - j2)(j) - 3(-1) + (3 + j2)(-j)] = 3; \end{aligned}$$

$$\begin{aligned} x[2] &= \frac{1}{4} [5 + (3 - j2)e^{j(2\pi(2)/4)} - 3e^{j(2\pi(2)(2)/4)} + (3 + j2)e^{j(2\pi(3)(2)/4)}] \\ &= \frac{1}{4} [5 + (3 - j2)(-1) - 3(1) + (3 + j2)(-1)] = -1; \end{aligned}$$

$$\begin{aligned} x[3] &= \frac{1}{4} [5 + (3 - j2)e^{j(2\pi(3)/4)} - 3e^{j(2\pi(2)(3)/4)} + (3 + j2)e^{j(2\pi(3)(3)/4)}] \\ &= \frac{1}{4} [5 + (3 - j2)(-j) - 3(-1) + (3 + j2)(j)] = 1. \end{aligned}$$

Examples 12.1 and 12.2 prove the following DFT pair:

$$x[k] = \begin{cases} 2 & k = 0 \\ 3 & k = 1 \\ -1 & k = 2 \\ 1 & k = 3 \end{cases} \xleftrightarrow{\text{DFT}} X[r] = \begin{cases} 5 & r = 0 \\ 3 - j2 & r = 1 \\ -3 & r = 2 \\ 3 + j2 & r = 3, \end{cases}$$

where both the DT sequence $x[k]$ and its DFT $X[r]$ are aperiodic with length $N = 4$.

Example 12.3

Calculate the N -point DFT of the aperiodic sequence $x[k]$ of length N , which is defined as follows:

$$x[k] = \begin{cases} 1 & 0 \leq k \leq (N_1 - 1) \\ 0 & N_1 \leq k \leq N. \end{cases}$$

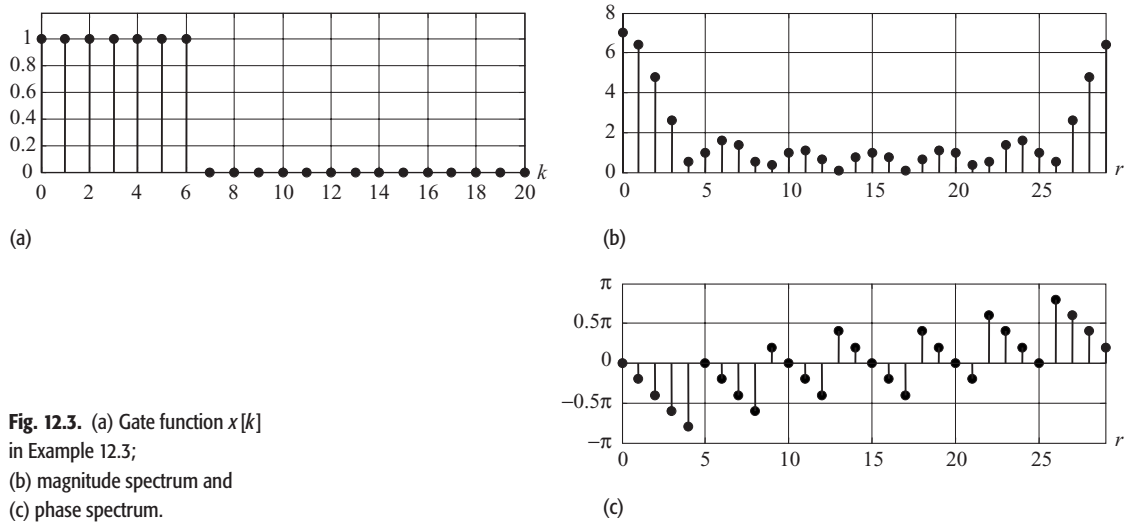


Fig. 12.3. (a) Gate function $x[k]$ in Example 12.3; (b) magnitude spectrum and (c) phase spectrum.

Solution

Using Eq. (12.14), the DFT of $x[k]$ is given by

$$\begin{aligned}
 X[r] &= \sum_{k=0}^{N-1} x[k]e^{-j(2\pi kr/N)} = \sum_{k=0}^{N_1-1} 1 \cdot e^{-j(2\pi kr/N)} \\
 &+ \sum_{k=N_1}^{N-1} 0 \cdot e^{-j(2\pi kr/N)} = \sum_{k=0}^{N_1-1} e^{-j(2\pi kr/N)},
 \end{aligned}$$

for $0 \leq r \leq (N-1)$. The right-hand side of this equation represents a GP series, which is as follows:

$$\begin{aligned}
 X[r] &= \sum_{k=0}^{N_1-1} e^{-j(2\pi kr/N)} = \begin{cases} N_1 & r = 0 \\ \frac{1 - e^{-j(2\pi r N_1/N)}}{1 - e^{-j(2\pi r/N)}} & r \neq 0 \end{cases} \\
 &= \begin{cases} N_1 & r = 0 \\ e^{-j(\pi r(N_1-1)/N)} \frac{\sin(\pi r N_1/N)}{\sin(\pi r/N)} & r \neq 0. \end{cases}
 \end{aligned}$$

Since $X[r]$ is a complex-valued function, its magnitude and phase components are given by

$$\begin{aligned}
 r = 0 \quad & |X[r]| = N_1 \quad \text{and} \quad \angle X[r] = 0; \\
 r \neq 0 \quad & |X[r]| = \frac{\sin(\pi r N_1/N)}{\sin(\pi r/N)} \quad \text{and} \quad \angle X[r] \\
 &= -\frac{\pi r(N_1 - 1)}{N} + \angle \sin(\pi r N_1/N) - \angle \sin(\pi r/N).
 \end{aligned}$$

The magnitude and phase spectra for $M = 7$ and length $N = 30$ are shown in Figs 12.3(b) and (c).

12.2.1 DFT as matrix multiplication

An alternative representation for computing the DFT is obtained by expanding Eq. (12.16) in terms of the time and frequency indices (k, r). For $N = M$, the resulting equations are expressed as follows:

$$\left. \begin{aligned}
 X[0] &= x[0] + x[1] + x[2] + \dots + x[N - 1], \\
 X[1] &= x[0] + x[1]e^{-j(2\pi/N)} + x[2]e^{-j(4\pi/N)} \\
 &\quad + \dots + x[N - 1]e^{-j(2(N-1)\pi/N)}, \\
 X[2] &= x[0] + x[1]e^{-j(4\pi/N)} + x[2]e^{-j(8\pi/N)} \\
 &\quad + \dots + x[N - 1]e^{-j(4(N-1)\pi/N)}, \\
 &\vdots \\
 X[N - 1] &= x[0] + x[1]e^{-j(2(N-1)\pi/N)} + x[2]e^{-j(4(N-1)\pi/N)} \\
 &\quad + \dots + x[N - 1]e^{-j(2(N-1)(N-1)\pi/N)},
 \end{aligned} \right\} \tag{12.18}$$

In the matrix-vector format they are given by

$$\underbrace{\begin{bmatrix} X[0] \\ X[1] \\ X[2] \\ \vdots \\ X[N - 1] \end{bmatrix}}_{\text{DFT vector: } \vec{X}} = \underbrace{\begin{bmatrix} 1 & 1 & 1 & \dots & 1 \\ 1 & e^{-j(2\pi/N)} & e^{-j(4\pi/N)} & \dots & e^{-j(2(N-1)\pi/N)} \\ 1 & e^{-j(4\pi/N)} & e^{-j(8\pi/N)} & \dots & e^{-j(4(N-1)\pi/N)} \\ \vdots & \vdots & \vdots & \ddots & \vdots \\ 1 & e^{-j(2(N-1)\pi/N)} & e^{-j(4(N-1)\pi/N)} & \dots & e^{-j(2(N-1)(N-1)\pi/N)} \end{bmatrix}}_{\text{DFT matrix: } F} \underbrace{\begin{bmatrix} x[0] \\ x[1] \\ x[2] \\ \vdots \\ x[N - 1] \end{bmatrix}}_{\text{signal vector: } \vec{x}}. \tag{12.19}$$

Equation (12.19) shows that the DFT coefficients $X[r]$ can be computed by left-multiplying the DT sequence $x[k]$, arranged in a column vector \vec{x} in ascending order with respect to the time index k , by the DFT matrix F .

Similarly, the expression for the inverse DFT given in Eq. (12.15) can be expressed as follows:

$$\underbrace{\begin{bmatrix} x[0] \\ x[1] \\ x[2] \\ \vdots \\ x[N - 1] \end{bmatrix}}_{\text{signal vector: } x} = \underbrace{\frac{1}{N} \begin{bmatrix} 1 & 1 & 1 & \dots & 1 \\ 1 & e^{j(2\pi/N)} & e^{j(4\pi/N)} & \dots & e^{j(2(N-1)\pi/N)} \\ 1 & e^{j(4\pi/N)} & e^{j(8\pi/N)} & \dots & e^{j(4(N-1)\pi/N)} \\ \vdots & \vdots & \vdots & \ddots & \vdots \\ 1 & e^{j(2(N-1)\pi/N)} & e^{j(4(N-1)\pi/N)} & \dots & e^{j(2(N-1)(N-1)\pi/N)} \end{bmatrix}}_{\text{DFT matrix: } G=F^{-1}} \underbrace{\begin{bmatrix} X[0] \\ X[1] \\ X[2] \\ \vdots \\ X[N - 1] \end{bmatrix}}_{\text{DFT vector: } X} \tag{12.20}$$

which implies that the DT sequence $x[k]$ can be obtained by left-multiplying the DFT coefficients $X[r]$, arranged in a column vector \vec{X} in ascending order

with respect to the DFT coefficient index r , by the inverse DFT matrix G and then scaling the result by a factor $1/N$. It is straightforward to show that $G \times F = F \times G = NI_N$, where I_N is the identity matrix of order N .

Example 12.4 repeats Example 12.1 using the matrix-vector representation for the DFT.

Example 12.4

Calculate the four-point DFT of the aperiodic signal $x[k]$ considered in Example 12.1.

Solution

Arranging the values of the DT sequence in the signal vector x , we obtain

$$x = [2 \quad 3 \quad -1 \quad 1]^T,$$

where superscript T represents the transpose operation for a vector. Using Eq. (12.19), we obtain

$$\begin{aligned} \begin{bmatrix} X[0] \\ X[1] \\ X[2] \\ X[3] \end{bmatrix} &= \underbrace{\begin{bmatrix} 1 & 1 & 1 & 1 \\ 1 & e^{-j(2\pi/N)} & e^{-j(4\pi/N)} & e^{-j(6\pi/N)} \\ 1 & e^{-j(4\pi/N)} & e^{-j(8\pi/N)} & e^{-j(12\pi/N)} \\ 1 & e^{-j(6\pi/N)} & e^{-j(12\pi/N)} & e^{-j(18\pi/N)} \end{bmatrix}}_{\text{DFT matrix: } F} \begin{bmatrix} x[0] \\ x[1] \\ x[2] \\ x[3] \end{bmatrix} \\ &= \underbrace{\begin{bmatrix} 1 & 1 & 1 & 1 \\ 1 & e^{-j(2\pi/N)} & e^{-j(4\pi/N)} & e^{-j(6\pi/N)} \\ 1 & e^{-j(4\pi/N)} & e^{-j(8\pi/N)} & e^{-j(12\pi/N)} \\ 1 & e^{-j(6\pi/N)} & e^{-j(12\pi/N)} & e^{-j(18\pi/N)} \end{bmatrix}}_{\text{DFT matrix: } F} \begin{bmatrix} 2 \\ 3 \\ -1 \\ 1 \end{bmatrix} = \begin{bmatrix} 5 \\ 3 - j2 \\ -3 \\ 3 + j2 \end{bmatrix}. \end{aligned}$$

The above values for the DFT coefficients are the same as the ones obtained in Example 12.1.

Example 12.5

Calculate the inverse DFT of $X[r]$ considered in Example 12.2.

Solution

Arranging the values of the DFT coefficients in the DFT vector x , we obtain

$$X = [5 \quad 3 - j2 \quad -3 \quad 3 + j2]^T.$$

Using Eq. (12.20), the DFT vector X is given by

$$\begin{aligned} \begin{bmatrix} x[0] \\ x[1] \\ x[2] \\ x[3] \end{bmatrix} &= \frac{1}{4} \begin{bmatrix} 1 & 1 & 1 & 1 \\ 1 & e^{j(2\pi/N)} & e^{j(4\pi/N)} & e^{j(6\pi/N)} \\ 1 & e^{j(4\pi/N)} & e^{j(8\pi/N)} & e^{j(12\pi/N)} \\ 1 & e^{j(6\pi/N)} & e^{j(12\pi/N)} & e^{j(18\pi/N)} \end{bmatrix} \begin{bmatrix} X[0] \\ X[1] \\ X[2] \\ X[3] \end{bmatrix} \\ &= \frac{1}{4} \begin{bmatrix} 1 & 1 & 1 & 1 \\ 1 & e^{j(2\pi/N)} & e^{j(4\pi/N)} & e^{j(6\pi/N)} \\ 1 & e^{j(4\pi/N)} & e^{j(8\pi/N)} & e^{j(12\pi/N)} \\ 1 & e^{j(6\pi/N)} & e^{j(12\pi/N)} & e^{j(18\pi/N)} \end{bmatrix} \begin{bmatrix} 5 \\ 3 - j2 \\ -3 \\ 3 + j2 \end{bmatrix} = \frac{1}{4} \begin{bmatrix} 8 \\ 12 \\ -4 \\ 4 \end{bmatrix} = \begin{bmatrix} 2 \\ 3 \\ -1 \\ 1 \end{bmatrix}. \end{aligned}$$

The above values for the DT sequence $x[k]$ are the same as the ones obtained in Example 12.2.

12.2.2 DFT basis functions

The matrix-vector representation of the DFT derived in Section 12.2.1 can be used to determine the set of basis functions for the DFT representation. Expressing Eq. (12.20) in the following format:

$$\begin{aligned} \begin{bmatrix} x[0] \\ x[1] \\ x[2] \\ \vdots \\ x[N-1] \end{bmatrix} &= \frac{1}{N} X[0] \begin{bmatrix} 1 \\ 1 \\ 1 \\ \vdots \\ 1 \end{bmatrix} + \frac{1}{N} X[1] \begin{bmatrix} 1 \\ e^{j(2\pi/N)} \\ e^{j(4\pi/N)} \\ \vdots \\ e^{j(2(N-1)\pi/N)} \end{bmatrix} + \frac{1}{N} X[2] \begin{bmatrix} 1 \\ e^{j(4\pi/N)} \\ e^{j(8\pi/N)} \\ \vdots \\ e^{j(4(N-1)\pi/N)} \end{bmatrix} \\ &+ \dots + \frac{1}{N} X[N-1] \begin{bmatrix} 1 \\ e^{j(2(N-1)\pi/N)} \\ e^{j(4(N-1)\pi/N)} \\ \vdots \\ e^{j(2(N-1)(N-1)\pi/N)} \end{bmatrix}, \end{aligned} \quad (12.21)$$

it is clear that the basis functions for the N -point DFT are given by the following set of vectors:

$$F_r = \frac{1}{N} \left[1 \quad \exp\left(j\frac{2\pi r}{N}\right) \quad \exp\left(j2\frac{2\pi r}{N}\right) \quad \dots \quad \exp\left(j(N-1)\frac{2\pi r}{N}\right) \right]^T,$$

for $0 \leq r \leq (N-1)$. Equation (12.21) illustrates that the DFT represents a DT sequence as a linear combination of complex exponentials, which are weighted by the corresponding DFT coefficients. Such a representation is useful for the analysis of linear, time-invariant systems.

As an example, Fig. 12.4 plots the real and imaginary components of the basis vectors for the eight-point DFT of an aperiodic sequence of length $N = 8$. From Fig. 12.4(a), we observe that the real components of the basis vectors correspond to a cosine function sampled at different sampling rates. Similarly, the imaginary components of the basis vectors correspond to a sine function

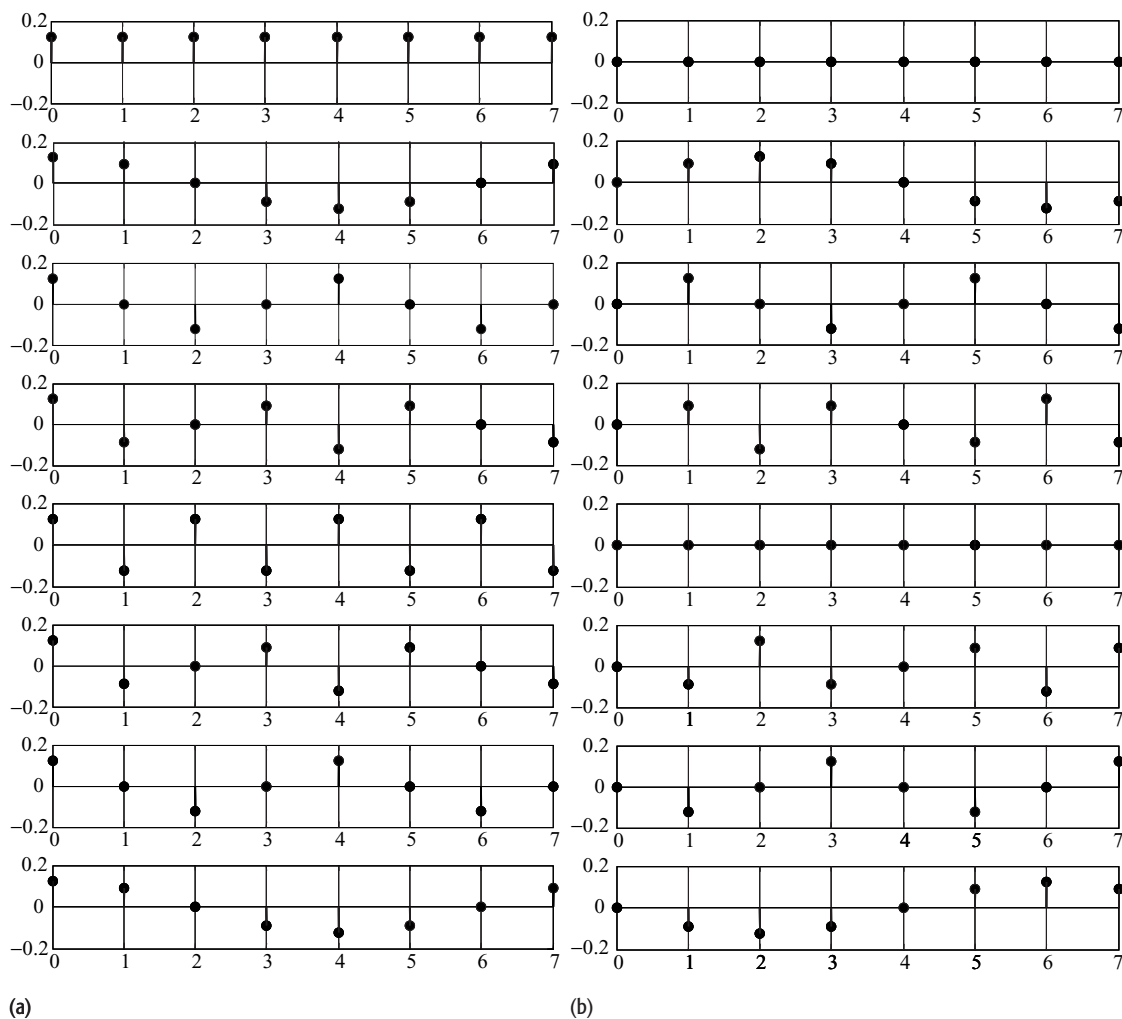


Fig. 12.4. Basis vectors for an eight-point DFT. (a) Real components; (b) imaginary components.

sampled at different sampling rates. This should not be surprising, since Euler’s identity expands a complex exponential as a complex sum between cosine and sine terms.

We now proceed with the estimation of the spectral content of both DT and CT signals using the DFT.

12.3 Spectrum analysis using the DFT

In this section, we illustrate how the DFT can be used to estimate the spectral content of the CT and DT signals. Examples 12.6–12.8 deal with the CT signals, while Examples 12.9 and 12.10 deal with the DT sequences.

Example 12.6

Using the DFT, estimate the frequency characteristics of the decaying exponential signal $g(t) = \exp(-0.5t)u(t)$. Plot the magnitude and phase spectra.

Solution

Following the procedure outlined in Section 12.1, the three steps involved in computing the CTFT are listed below.

Step 1: Impulse-train sampling Based on Table 5.1, the CTFT of the decaying exponential is given by

$$g(t) = e^{-0.5t}u(t) \xrightarrow{\text{CTFT}} G(\omega) = \frac{1}{0.5 + j\omega}.$$

This CTFT pair implies that the bandwidth of $g(t)$ is infinite. Ideally speaking, the Nyquist sampling theorem can never be satisfied for the decaying exponential signal. However, we exploit the fact that the magnitude $|G(\omega)|$ of the CTFT decreases monotonically with higher frequencies and we neglect any frequency components at which the magnitude falls below a certain threshold η . Selecting the value of $\eta = 0.01 \times |G(\omega)|_{\max}$, the threshold frequency B is given by

$$\left| \frac{1}{0.5 + j2\pi B} \right| \leq 0.01 \times |G(\omega)|_{\max}.$$

Since the maximum value of the magnitude $|G(\omega)|$ is 2 at $\omega = 0$, the above expression reduces to

$$\sqrt{0.25 + (2\pi B)^2} \geq 50,$$

or $B \geq 7.95$ Hz. The Nyquist sampling rate f_1 is therefore given by

$$f_1 \geq 2 \times 7.95 = 15.90 \text{ samples/s.}$$

Selecting a sampling rate of $f_1 = 20$ samples/s, or a sampling interval $T_1 = 1/20 = 0.05$ s, the DT approximation of the decaying exponential is given by

$$g[k] = g(kT_1) = e^{-0.5kT_1}u[k] = e^{-0.025k}u[k].$$

Since there is a discontinuity at $k = 0$, we set $g[0] = 0.5$.

Step 2: Time-limitation To truncate the length of $g[k]$, we apply a rectangular window of length $N = 203$ samples. The truncated sequence is given by

$$g_w[k] = e^{-0.025k}(u[k] - u[k - 199]) = \begin{cases} e^{-0.025k} & 0 \leq k \leq 202 \\ 0 & \text{elsewhere.} \end{cases}$$

The subscript w in $g_w[k]$ denotes the truncated version of $g[k]$ obtained by multiplying by the window function $w[k]$. Note that the truncated sequence $g_w[k]$ is a fairly good approximation of $g[k]$, as the peak magnitude of the truncated samples is given by 0.0063 and occurs at $k = 203$. This is only 0.63% of the peak value of the complex exponential $g[k]$.

Step 3: DFT computation The DFT of the truncated DT sequence $g_w[k]$ can now be computed directly from Eq. (12.16). MATLAB provides a built-in function `fft`, which has the calling syntax of

```
>> G = fft(g);
```

where g is the signal vector containing the values of the DT sequence $g_w[k]$ and G is the computed DFT. Both g and G have a length of N , implying that an N -point DFT is being taken. The built-in function `fft` computes the DFT within the frequency range $0 \leq r \leq (N-1)$. Since the DFT is periodic, we can obtain the DFT within the frequency range $-(N-1)/2 \leq r \leq (N-1)/2$ by a circular shift of the DFT coefficients. In MATLAB, this is accomplished by the `fftshift` function.

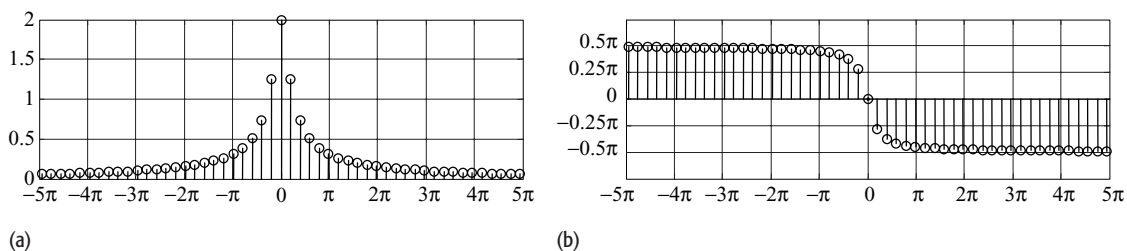
Having computed the DFT, we use Eq. (12.12) to estimate the CTFT of the original CT decaying exponential signal $g(t)$. The MATLAB code for computing the CTFT is as follows:

```
>> f1 = 20; t1 = 1/f1; % set sampling rate and interval
>> N = 203; k = 0:N-1; % set length of DT sequence to
                        N = 203
>> g = exp(-0.025*k); % compute the DT sequence
    g(1) = 0.5;
>> G = fft(g); % determine the 203-point DFT
>> G = fftshift(G); % shift the DFT coefficients
>> G = t1*G; % scale DFT such that DFT = CTFT
>> w = -pi*f1:2*pi*f1/N:pi*f1-2*pi*f1/N; %compute CTFT
    frequencies
>> stem(w,abs(G)); % plot CTFT magnitude spectrum
>> stem(w,angle(G)); % plot CTFT phase spectrum
```

Fig. 12.5. Spectral estimation of decaying exponential signal $g(t) = \exp(-0.5t)u(t)$ using the DFT in Example 12.6. (a) Estimated magnitude spectrum; (b) estimated phase spectrum.

The resulting plots are shown in Fig. 12.5, where we have limited the frequency axis to the range $-5\pi \leq \omega \leq 5\pi$. The magnitude and phase spectra plotted in Fig. 12.5 are fairly good estimates of the frequency characteristics of the decaying exponential signal listed in Table 5.3.

In Example 12.6, we used the CTFT $G(\omega)$ to determine the appropriate sampling rate. In most practical situations, however, the CTFTs are not known



12 Discrete Fourier transform

and one is forced to make an intelligent estimate of the bandwidth of the signal. If the frequency and time characteristics of the signal are not known, a high sampling rate and a large time window are arbitrarily chosen. In such cases, it is advised that a number of sampling rates and lengths be tried before finalizing the estimates.

Example 12.7

Using the DFT, estimate the frequency characteristics of the CT signal $h(t) = 2\exp(j18\pi t) + \exp(-j8\pi t)$.

Solution

Following the procedure outlined in Section 12.1, the three steps involved in computing the CTFT are as follows.

Step 1: Impulse-train sampling The CT signal $h(t)$ consists of two complex exponentials with fundamental frequencies of 9 Hz and 4 Hz. The Nyquist sampling rate f_1 is therefore given by

$$f_1 \geq 2 \times 9 = 18 \text{ samples/s.}$$

We select a sampling rate of $f_1 = 32$ samples/s, or a sampling interval $T_1 = 1/32$ s. The DT approximation of $h(t)$ is given by

$$h[k] = h(kT_1) = 2e^{j18\pi k/32} + e^{-j8\pi k/32}.$$

Step 2: Time-limitation The DT sequence $h[k]$ is a periodic signal with fundamental period $K_0 = 32$. For periodic signals, it is sufficient to select the length of the rectangular window equal to the fundamental period. Therefore, N is set to 32.

Step 3: DFT computation The MATLAB code for computing the DFT of the truncated DT sequence is as follows.

```
>> f1 = 32; t1 = 1/f1;           % set sampling rate and
                                interval
>> N = 32; k = 0:N-1;           % set length of DT sequence
                                to N = 32
>> h = 2*exp(j*18*pi*k/32) + exp(-j*8*pi*k/32); % compute
                                the DT sequence
>> H = fft(h);                  % determine the 32-point DFT
>> H = fftshift(H);             % shift the DFT coefficients
>> H = t1*H;                    % scale DFT such that DFT =
                                CTFT
```

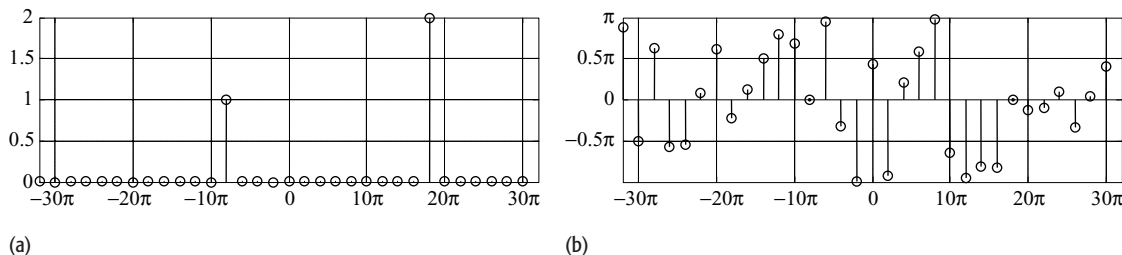


Fig. 12.6. Spectral estimation of decaying exponential signal $h(t) = 2\exp(j18\pi t) + \exp(-j8\pi t)$ using the DFT in Example 12.7. (a) Estimated magnitude spectrum; (b) estimated phase spectrum.

```
>> w = -pi*f1:2*pi*f1/N:pi *f1-2*pi*f1/N; % compute CTFT
    frequencies
>> stem(w, abs(H) ); % plot CTFT magnitude spectrum
>> stem(w, angle(H) ); % plot CTFT phase spectrum
```

The resulting plots are shown in Fig. 12.6, and they have a frequency resolution of $\Delta\omega = 2\pi$. We know that the CTFT for $h(t)$ is given by

$$2e^{j18\pi t} + e^{-j8\pi t} \xrightarrow{\text{CTFT}} 2\delta(\omega - 18\pi) + \delta(\omega + 8\pi).$$

We observe that the two impulses at $\omega = -8\pi$ and 18π radians/s are accurately estimated in the magnitude spectrum plotted in Fig. 12.6(a). Also, the relative amplitude of the two impulses corresponds correctly to the area enclosed by these impulses in the CTFT for $h(t)$.

The phase spectrum plotted in Fig. 12.6(b) is unreliable except for the two frequencies $\omega = -8\pi$ and 18π radians/s. At all other frequencies, the magnitude $|H(\omega)|$ is zero, therefore the phase $\angle H(\omega)$ carries no information for the following reason. The phase is computed as the inverse tangent of the ratio between the imaginary and real components of $H(\omega)$. When $|H(\omega)|$ is close to zero, the argument of the inverse tangent is given by ϵ_1/ϵ_2 , with ϵ_1 and ϵ_2 approaching zero. In such cases, incorrect results are obtained for the phase. The phase $\angle H(\omega)$ is therefore ignored when $|H(\omega)|$ is close to zero.

Example 12.8

Using the DFT, estimate the frequency characteristics of the CT signal $x(t) = 2\exp(j19\pi t)$.

Solution

Following the procedure outlined in Section 12.1, the three steps involved in computing the CTFT are as follows

Step 1: Impulse-train sampling The CT signal $x(t)$ constitutes a complex exponential with fundamental frequency 9.5 Hz. The Nyquist sampling rate f_1 is therefore given by

$$f_1 \geq 2 \times 9.5 = 19 \text{ samples/s.}$$

12 Discrete Fourier transform

As in Example 12.7, we select a sampling rate of $f_1 = 32$ samples/s, or a sampling interval $T_1 = 1/32$ s. The DT approximation of $h(t)$ is given by

$$x[k] = x(kT_1) = 2e^{j19\pi k/32}.$$

Step 2: Time-limitation Since the DT sequence $h[k]$ is a periodic signal with fundamental period $K_0 = 32$, the length N of the rectangular window is set to 32.

Step 3: DFT computation The MATLAB code for computing the DFT of the truncated DT sequence is as follows:

```
>> f1 = 32; t1 = 1/f1;           % set sampling rate and
                                interval
>> N = 32; k = 0:N-1;           % set length of DT sequence to
                                N = 32
>> x = 2*exp(j*19*pi*k/32); % compute the DT sequence
>> X = fft(x);                   % determine the 32-point DFT
>> X = fftshift(X);              % shift the DFT coefficients
>> X = t1*X;                     % scale DFT such that DFT =
                                CTFT
>> w = -pi*f1:2*pi*f1/N: pi*f1-2*pi*f1/N; % compute CTFT
                                frequencies
>> stem(w,abs(X));               % plot CTFT magnitude spectrum
```

The resulting magnitude spectrum is shown in Fig. 12.7(a), which has a frequency resolution of $\Delta\omega = 2\pi$ radians/s. Comparing with the CTFT for $x(t)$, which is given by

$$2e^{j19\pi t} \xrightarrow{\text{CTFT}} 2\delta(\omega - 19\pi),$$

we observe that Fig. 12.7(a) provides us with an erroneous result. This error is attributed to the poor resolution $\Delta\omega$ chosen to frequency-sample the CTFT. Since $\Delta\omega = 2\pi$, the frequency component of 19π present in $x(t)$ cannot be displayed accurately at the selected resolution. In such cases, the strength of the frequency component of 19π radians/s leaks into the adjacent frequencies, leading to non-zero values at these frequencies. This phenomenon is referred to as the picket fence effect.

Figure 12.7(b) plots the magnitude spectrum when the number N of samples in the discretized sequence is increased to 64. Since `fft` uses the same number M of samples to discretize the CTFT, the resolution $\Delta\omega = 2\pi T_1/M = \pi$ radians/s. The MATLAB code for estimating the CTFT is as follows:

```
>> f1 = 32; t1 = 1/f1; % set sampling rate and interval
>> N = 64; k = 0:N-1; % set length of DT sequence
                                to N = 64
```

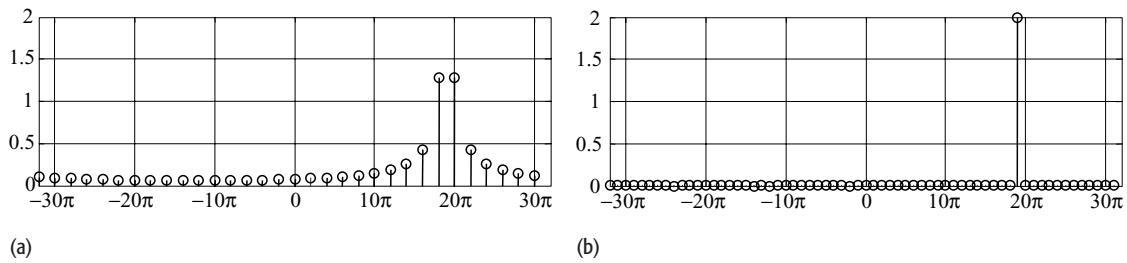


Fig. 12.7. Spectral estimation of complex exponential signal $x(t) = 2\exp(j19\pi t)$ using the DFT in Example 12.8.
 (a) Estimated magnitude spectrum, with a 32-point DFT.
 (b) Same as part (a) except that a 64-point DFT is computed.

```
>> x = 2*exp(j*19*pi*k/32); % compute the DT sequence
>> X = fft(x); % determine the 64-point DFT
>> X = fftshift(X); % shift the DFT coefficients
>> X = 0.5*t1*X; % scale DFT such that DFT =
                CTFT
>> w = -pi*f1:2*pi*f1/N:pi*f1-2*pi*f1/N; % compute CTFT
        frequencies
>> stem(w,abs(X)); % plot CTFT magnitude spectrum
```

In the above code, we have highlighted the commands that have been changed from the original version. In addition to setting the length N to 64 in the above code, we also note that the magnitude of the CTFT X is now being scaled by a factor $0.5 \times T_1$. The additional factor of 0.5 is introduced because we are now computing the DFT over two consecutive periods of the periodic sequence $x[k]$. Doubling the time duration doubles the values of the DFT coefficients, so a factor of 0.5 is introduced to compensate for the increase. Figure 12.7(b), obtained using a 64-point DFT, is a better estimate for the magnitude spectrum of $x(t)$ than Fig. 12.7(a), obtained using a 32-point DFT.

The DFT can also be used to estimate the DTFT of DT sequences. Examples 12.9 and 12.10 compute the DTFT of two aperiodic sequences.

Example 12.9

Using the DFT, calculate the DTFT of the DT decaying exponential sequence $x[k] = 0.6^k u[k]$.

Solution

Estimating the DTFT involves only Steps 2 and 3 outlined in Section 12.1.

Step 2: Time-limitation Applying a rectangular window of length $N = 10$, the truncated sequence is given by

$$x_w[k] = \begin{cases} 0.6^k & 0 \leq k \leq 9 \\ 0 & \text{elsewhere.} \end{cases}$$

Table 12.1. Comparison between the DFT and DTFT coefficients in Example 12.9

DFT index, r	DTFT frequency, $\Omega_r = 2\pi r/N$	DFT coefficients, $X[r]$	DTFT coefficients, $X(\Omega)$
-5	$-\pi$	0.6212	0.6250
-4	-0.8π	$0.6334 + j0.1504$	$0.6373 + j0.1513$
-3	-0.6π	$0.6807 + j0.3277$	$0.6849 + j0.3297$
-2	-0.4π	$0.8185 + j0.5734$	$0.8235 + j0.5769$
-1	-0.2π	$1.3142 + j0.9007$	$1.3222 + j0.9062$
0	0	2.4848	2.5000
1	0.2π	$1.3142 - j0.9007$	$1.3222 - j0.9062$
2	0.4π	$0.8185 - j0.5734$	$0.8235 - j0.5769$
3	0.6π	$0.6807 - j0.3277$	$0.6849 - j0.3297$
4	0.8π	$0.6334 - j0.1504$	$0.6373 - j0.1513$

Step 3: DFT computation The MATLAB code for computing the DFT is as follows:

```
>> N = 10; k = 0:N-1;           % set length of DT sequence
                                % to N = 10
>> x = 0.6.^k;                 % compute the DT sequence
>> X = fft(x);                 % determine the 201-point DFT
>> X = fftshift(X);           % shift the DFT coefficients
>> w = -pi:2*pi/N:pi-2*pi/N; % compute DTFT frequencies
```

Table 12.1 compares the computed DFT coefficients with the corresponding DTFT coefficients obtained from the following DTFT pair:

$$0.6^k u[k] \xleftrightarrow{\text{CTFT}} \frac{1}{1 - 0.6e^{-j\Omega}}$$

We observe that the values of the DFT coefficients are fairly close to the DTFT values.

Example 12.10

Calculate the DTFT of the aperiodic sequence $x[k] = [2, 1, 0, 1]$ for $0 \leq k \leq 3$.

Solution

Using Eq. (12.6), the DFT coefficients are given by

$$X[r] = [4, 2, 0, 2] \quad \text{for } 0 \leq r \leq 3.$$

Mapping in the DTFT domain, the corresponding DTFT coefficients are given by

$$X(\Omega_r) = [4, 2, 0, 2] \quad \text{for } \Omega_r = [0, 0.5\pi, \pi, 1.5\pi] \text{ radians/s.}$$

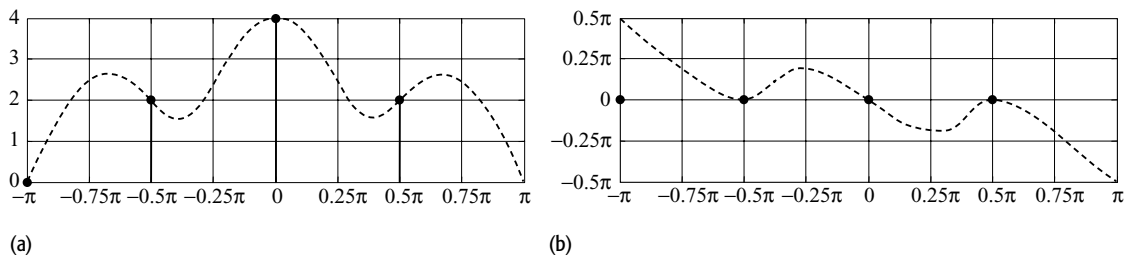


Fig. 12.8. Spectral estimation of DT sequences using the DFT in Example 12.10. (a) Estimated magnitude spectrum; (b) estimated phase spectrum. The dashed lines show the continuous spectrum obtained from the DTFT.

If instead the DTFT is to be plotted within the range $-\pi \leq \Omega \leq \pi$, then the DTFT coefficients can be rearranged as follows:

$$X(\Omega_r) = [4, 2, 0, 2] \quad \text{for} \quad \Omega_r = [-\pi, -0.5\pi, 0, 0.5\pi] \text{ radians/s.}$$

The magnitude and phase spectra obtained from the DTFT coefficients are sketched using bar plots in Figs 12.8(a) and (b). For comparison, we use Eq. (11.27b) to derive the DTFT for $x[k]$. The DTFT is given by

$$X(\Omega) = \sum_{k=0}^3 x[k]e^{-j\Omega k} = 2 + e^{-j\Omega} + e^{-j3\Omega}.$$

The actual magnitude and phase spectra based on the above DTFT expression are plotted in Figs 12.8(a) and (b) respectively (see dashed lines). Although the DFT coefficients provide exact values of the DTFT at the discrete frequencies $\Omega_r = [0, 0.5\pi, \pi, 1.5\pi]$ radians/s, no information is available on the characteristics of the magnitude and phase spectra for the intermediate frequencies. This is a consequence of the low resolution used by the DFT to discretize the DTFT frequency Ω . Section 12.3.1 introduces the concept of zero padding, which allows us to improve the resolution used by the DFT.

12.3.1 Zero padding

To improve the resolution of the frequency axis Ω in the DFT domain, a commonly used approach is to append the DT sequences with additional zero-valued samples. This process is called zero padding, and for an aperiodic sequence $x[k]$ of length N is defined as follows:

$$x_{zp}[k] = \begin{cases} x[k] & 0 \leq k \leq (N - 1) \\ 0 & N \leq k \leq (M - 1). \end{cases}$$

The zero-padded sequence $x_{zp}[k]$ has an increased length of M . The frequency resolution $\Delta\Omega$ of the zero-padded sequence is improved from $2\pi/N$ to $2\pi/M$. Example 12.11 illustrates the improvement in the DTFT achieved with the zero-padding approach.

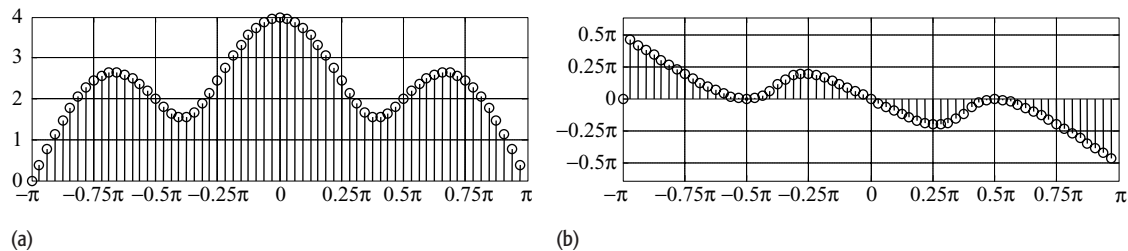


Fig. 12.9. Spectral estimation of zero-padded DT sequences using the DFT in Example 12.11. (a) Estimated magnitude spectrum; (b) estimated phase spectrum.

Example 12.11

Compute the DTFT of the aperiodic sequence $x[k] = [2, 1, 0, 1]$ for $0 \leq k \leq 3$ by padding 60 zero-valued samples at the end of the sequence.

Solution

The MATLAB code for computing the DTFT of the zero-padded sequence is as follows:

```
>> N = 64; k = 0:N-1;           % set length of DT sequence
                                % to N = 64
>> x = [2 1 0 1 zeros(1,60)]; % compute the DT sequence
>> X = fft(x);                 % determine the 64-point DFT
>> X = fftshift(X);           % shift the DFT coefficients
>> w = -pi:2*pi/N:pi-2*pi/N; % compute DTFT frequencies
>> stem(w,abs(X));            % plot the magnitude
                                % spectrum
>> stem(w,angle(X));         % plot the phase spectrum
```

The magnitude and phase spectra of the zero-padded sequence are plotted in Figs 12.9(a) and (b), respectively. Compared with Fig. 12.8, we observe that the estimated spectra in Fig. 12.9 provide an improved resolution and better estimates for the frequency characteristics of the DT sequence.

12.4 Properties of the DFT

In this section, we present the properties of the M -point DFT. The length of the DT sequence is assumed to be $N \leq M$. For $N < M$, the DT sequence is zero-padded with $M - N$ zero-valued samples. The DFT properties presented below are similar to the corresponding properties for the DTFT discussed in Chapter 11.

12.4.1 Periodicity

The M -point DFT of an aperiodic DT sequence with length N with $M \geq N$ is itself periodic with period M . In other words,

$$X[r] = X[r + pM], \quad (12.22)$$

for $0 \leq r \leq (M - 1)$ with $p \in R^+$.

12.4.2 Orthogonality

The column vectors F_r of the DFT matrix F , defined in Eq. (12.21), form the basis vectors of the DFT and are orthogonal with respect to each other such that

$$F_r^H \cdot F_q = \begin{cases} M & \text{for } r = q \\ 0 & \text{for } r \neq q, \end{cases}$$

where (\cdot) represents the dot product and the superscript H represents the Hermitian operation.

12.4.3 Linearity

If $x_1[k]$ and $x_2[k]$ are two DT sequences with the following M -point DFT pairs:

$$x_1[k] \xleftrightarrow{\text{DFT}} X_1[r] \text{ and } x_2[k] \xleftrightarrow{\text{DFT}} X_2[r],$$

then the linearity property states that

$$a_1x_1[k] + a_2x_2[k] \xleftrightarrow{\text{DFT}} a_1X_1[r] + a_2X_2[r], \quad (12.23)$$

for any arbitrary constants a_1 and a_2 , which may be complex-valued.

12.4.4 Hermitian symmetry

The M -point DFT $X[r]$ of a real-valued aperiodic sequence $x[k]$ is conjugate-symmetric about $r = M/2$. Mathematically, the Hermitian symmetry implies that

$$X[r] = X^*[M - r], \quad (12.24)$$

where $X^*[r]$ denotes the complex conjugate of $X[r]$.

In terms of the magnitude and phase spectra of the DFT $X[r]$, the Hermitian symmetry property can be expressed as follows:

$$|X[M - r]| = |X[r]| \quad \text{and} \quad \angle X[M - r] = -\angle X[r], \quad (12.25)$$

implying that the magnitude spectrum is even and that the phase spectrum is odd.

The validity of the Hermitian symmetry can be observed in the DFT plotted for various aperiodic sequences in Examples 12.2–12.11.

12.4.5 Time shifting

If $x[k] \xleftrightarrow{\text{DFT}} X[r]$, then

$$x[k - k_0] \xleftrightarrow{\text{DFT}} e^{-j2\pi k_0 r/M} X[r] \quad (12.26)$$

for an M -point DFT and any arbitrary integer k_0 .

12.4.6 Circular convolution

If $x_1[k]$ and $x_2[k]$ are two DT sequences with the following M -point DFT pairs:

$$x_1[k] \xleftrightarrow{\text{DFT}} X_1[r] \quad \text{and} \quad x_2[k] \xleftrightarrow{\text{DFT}} X_2[r],$$

then the circular convolution property states that

$$x_1[k] \otimes x_2[k] \xleftrightarrow{\text{DFT}} X_1[r]X_2[r] \quad (12.27)$$

and

$$x_1[k]x_2[k] \xleftrightarrow{\text{DFT}} \frac{1}{M}[X_1[r] \otimes X_2[r]], \quad (12.28)$$

where \otimes denotes the circular convolution operation. Note that the two sequences must have the same length in order to compute the circular convolution.

Example 12.12

In Example 10.11, we calculated the circular convolution $y[k]$ of the two aperiodic sequences $x[k] = [0, 1, 2, 3]$ and $h[k] = [5, 5, 0, 0]$ defined over $0 \leq k \leq 3$. Recalculate the result of the circular convolution using the DFT convolution property.

Solution

The four-point DFTs of the aperiodic sequences $x[k]$ and $h[k]$ are given by

$$X[r] = [6, -2 + j2, -2, -2 - j2]$$

and

$$H[r] = [10, 5 - j5, 0, 5 + j5]$$

for $0 \leq r \leq 3$. Using Eq. (12.27), the four-point DFT of the circular convolution between $x[k]$ and $h[k]$ is given by

$$x_1[k] \otimes x_2[k] \xleftrightarrow{\text{DFT}} [60, j20, 0 - j20].$$

Taking the inverse DFT, we obtain

$$x_1[k] \otimes x_2[k] = [15, 5, 15, 25],$$

which is identical to the answer obtained in Example 10.11.

12.4.7 Parseval's theorem

If $x[k] \xrightarrow{\text{DFT}} X[r]$, then the energy of the aperiodic sequence $x[k]$ of length N can be expressed in terms of its M -point DFT as follows:

$$E_x = \sum_{k=0}^{N-1} |x[k]|^2 = \frac{1}{M} \sum_{k=0}^{M-1} |X[r]|^2. \quad (12.29)$$

Parseval's theorem shows that the DFT preserves the energy of the signal within a scale factor of M .

12.5 Convolution using the DFT

In Section 10.6.1, we showed that the linear convolution $x_1[k] * x_2[k]$ between two time-limited DT sequences $x_1[k]$ and $x_2[k]$ of lengths K_1 and K_2 , respectively, can be expressed in terms of the circular convolution $x_1[k] \otimes x_2[k]$. The procedure requires zero padding both $x_1[k]$ and $x_2[k]$ to have individual lengths of $K \geq (K_1 + K_2 - 1)$. It was shown that the result of the circular convolution of the zero-padded sequences is the same as that of the linear convolution.

Since computationally efficient algorithms are available for computing the DFT of a finite-duration sequence, the circular convolution property can be exploited to implement the linear convolution of the two sequences $x_1[k]$ and $x_2[k]$ using the following procedure.

- (1) Compute the K -point DFTs $X_1[r]$ and $X_2[r]$ of the two time-limited sequences $x_1[k]$ and $x_2[k]$. The value of K is lower bounded by $(K_1 + K_2 - 1)$, i.e. $K \geq (K_1 + K_2 - 1)$.
- (2) Compute the product $X_3[r] = X_1[r]X_2[r]$ for $0 \leq r \leq K - 1$.
- (3) Compute the sequence $x_3[k]$ as the inverse DFT of $X_3[r]$. The resulting sequence $x_3[k]$ is the result of the linear convolution between $x_1[k]$ and $x_2[k]$.

The above approach is explained in Example 12.13.

Example 12.13

Example 10.13 computed the linear convolution of the following DT sequences:

$$x[k] = \begin{cases} 2 & k = 0 \\ -1 & |k| = 1 \\ 0 & \text{otherwise} \end{cases} \quad \text{and} \quad h[k] = \begin{cases} 2 & k = 0 \\ 3 & |k| = 1 \\ -1 & |k| = 2 \\ 0 & \text{otherwise,} \end{cases}$$

using the circular convolution method outlined in Algorithm 10.4 in Section 10.6.1. Repeat Example 10.13 using the DFT-based approach described above.

12 Discrete Fourier transform

Table 12.2. Values of $X'[r]$, $H'[r]$ and $Y[r]$ for $0 \leq r \leq 6$ in Example 12.13

r	$X'[r]$	$H'[r]$	$Y'[r]$
0	0	6	0
1	0.470 - j0.589	-1.377 - j6.031	-4.199 - j2.024
2	-5.44 - j2.384	-2.223 + j1.070	3.760 + j4.178
3	-3.425 - j1.650	-2.901 - j3.638	3.933 + j17.247
4	-3.425 + j1.650	-2.901 + j3.638	3.933 - j17.247
5	-0.544 + j2.384	-2.223 - j1.070	3.760 - j4.178
6	0.470 + j0.589	-1.377 + j6.031	-4.199 + j2.024

Solution

Step 1 Since the sequences $x[k]$ and $h[k]$ have lengths $K_x = 5$ and $K_y = 3$, the value of $K \geq (5 + 3 - 1) = 7$. We set $K = 7$ in this example:

$$\begin{aligned} \text{padding } (K - K_x) = 4 \text{ additional zeros to } x[k], \text{ we obtain } x'[k] \\ = [-1 \ 2 \ -1 \ 0 \ 0 \ 0 \ 0]; \\ \text{padding } (K - K_h) = 2 \text{ additional zeros to } h[k], \text{ we obtain } h'[k] \\ = [-1 \ 3 \ 2 \ 3 \ -1 \ 0 \ 0]. \end{aligned}$$

The DFTs of $x'[k]$ are shown in the second column of Table 12.2, where the values for $X'[r]$ have been rounded off to three decimal places. Similarly, the DFTs of $h'[k]$ are shown in the third column of Table 12.2.

Step 2 The value of $Y[r] = X'[r]H'[r]$, for $0 \leq r \leq 6$, are shown in the fourth column of Table 12.2

Step 3 Taking the inverse DFT of $Y[r]$ yields

$$Y[k] = [0.998 \quad -5 \quad 5.001 \quad -1.999 \quad 5 \quad -5.002 \quad 1.001].$$

Except for approximation errors caused by the numerical precision of the computer, the above results are the same as those obtained from the direct computation of the linear convolution included in Example 10.13.

12.5.1 Computational complexity

We now compare the computational complexity of the time-domain and DFT-based implementations of the linear convolution between the time-limited

sequences $x_1[k]$ and $x_2[k]$ with lengths K_1 and K_2 , respectively. For simplicity, we assume that $x_1[k]$ and $x_2[k]$ are real-valued sequences with lengths K_1 and K_2 , respectively.

Time-domain approach This is based on the direct computation of the convolution sum

$$y[k] = x_1[k] * x_2[k] = \sum_{m=-\infty}^{\infty} x_1[m]x_2[k - m],$$

which requires roughly $K_1 \times K_2$ multiplications and $K_1 \times K_2$ additions. The total number of floating point operations (flops) required with the time-domain approach is therefore given by $2K_1 \times K_2$.

DFT-based approach Step 1 of the DFT-based approach computes two $K = K_1 + K_2 - 1$ point DFTs of the DT sequences $x_1[k]$ and $x_2[k]$. In Section 12.6, we show that a K -point DFT can be implemented using fast Fourier transform (FFT) techniques with $0.5K \log_2 K$ complex multiplications and $K \log_2 K$ complex additions. Since each complex multiplication requires four scalar multiplications and two scalar additions, a total of six flops are required per complex multiplication. Each complex addition, on the other hand, requires two scalar additions, leading to two flops per complex addition. Therefore, Step 1 of the DFT-based approach requires a total of $2 \times [3K \log_2 K + 2K \log_2 K] = 10K \log_2 K$ flops.

Step 2 multiplies DFTs for $x_1[k]$ and $x_2[k]$. Each DFT has a length of $K = K_1 + K_2 - 1$ points; therefore, a total of K complex multiplications and $K - 1 \approx K$ complex additions are required. The total number of computations required in Step 1 is therefore given by $8K$ or $8(K_1 + K_2 - 1)$ flops.

Step 3 computes one inverse DFT based on the FFT implementation requiring $5K \log_2 K$ flops.

The total number of flops required with the DFT-based approach is therefore given by

$$15K \log_2 K + 6K \approx 15K \log_2 K \text{ flops,}$$

where $K = K_1 + K_2 - 1$. Assuming $K_1 = K_2$, the DFT-based approach provides a computation saving of $O(\log_2 K/K)$ in comparison with the direct computation of the convolution sum in the time domain. Table 12.3 compares the computational complexity of the two approaches for a few selected values of K_1 and K_2 . We observe that for sequences with lengths greater than 1000 samples, the DFT-based approach provides significant savings over the direct computation of the circular convolution in the time domain.

Table 12.3. Comparison of the computational complexities of the time-domain versus the DFT-based approaches used to compute the linear convolution

Length K_1 of $x_1[k]$	Length K_2 of $x_2[k]$	Computational complexity, flops	
		Time domain ($2K_1 \times K_2$ flops)	DFT ($15K \log_2 K$ flops)
32	5	320	2792
32	16	1024	3916
32	32	2048	5649
1000	5	10 000	150 171
1000	200	400 000	183 943
1000	1000	2 000 000	328 787

12.6 Fast Fourier transform

There are several well known techniques including the radix-2, radix-4, split radix, Winograd, and prime factor algorithms that are used for computing the DFT. These algorithms are referred to as the fast Fourier transform (FFT) algorithms. In this section, we explain the radix-2 decimation-in-time FFT algorithm.

To provide a general frame of reference, let us consider the computational complexity of the direct implementation of the K -point DFT for the time-limited sequence $x[k]$ with length K . Based on its definition,

$$X[r] = \sum_{k=0}^{K-1} x[k] e^{-j(2\pi kr/K)}, \quad (12.30)$$

K complex multiplications and $K-1$ complex additions are required to compute a single DFT coefficient. Computation of all K DFT coefficients requires K^2 complex additions and K^2 complex multiplications, where we have assumed K to be large such that $K-1 \approx K$.

In terms of flops, each complex multiplication requires four scalar multiplications and two scalar additions, and each complex addition requires two scalar additions. Computation of a single DFT coefficient, therefore, requires $8K$ flops. The total number of scalar operations for computing the complete DFT is given by $8K^2$ flops.

We now proceed with the radix-2 FFT decimation-in-time algorithm. The radix-2 algorithm is based on the following principle.

Proposition 12.1 *For even values of K , the K -point DFT of a real-valued sequence $x[k]$ with length $M \leq K$ can be computed from the DFT coefficients of two subsequences: (i) $x[2k]$, containing the even-valued samples of $x[k]$, and (ii) $x[2k+1]$, containing the odd-valued samples of $x[k]$.*

Proof

Expressing Eq. (12.30) in terms of real- and odd-numbered-valued samples of $x[k]$, we obtain

$$X[r] = \underbrace{\sum_{k=0,2,4,\dots}^{K-1} x[k]e^{-j(2\pi kr/K)}}_{\text{Term I}} + \underbrace{\sum_{k=1,3,5,\dots}^{K-1} x[k]e^{-j(2\pi kr/K)}}_{\text{Term II}}, \quad (12.31)$$

for $0 \leq r \leq (M - 1)$. Substituting $k = 2m$ in Term I and $k = 2m + 1$ in Term II, Eq. (12.31) can be expressed as follows:

$$X[r] = \sum_{m=0,1,2,\dots}^{K/2-1} x[2m]e^{-j(2\pi(2m)r/K)} + \sum_{m=0,1,2,\dots}^{K/2-1} x[2m + 1]e^{-j(2\pi(2m+1)r/K)}$$

or

$$X[r] = \sum_{m=0,1,2,\dots}^{K/2-1} x[2m]e^{-j(2\pi mr/(K/2))} + e^{-j(2\pi r/K)} \sum_{m=0,1,2,\dots}^{K/2-1} x[2m + 1]e^{-j(2\pi mr/(K/2))}, \quad (12.32)$$

where $\exp[-j2\pi(2m)r/K] = \exp[-j2\pi mr/(K/2)]$. By expressing $g[m] = x[2m]$ and $h[m] = x[2m + 1]$, we can express Eq. (12.32) in terms of the DFTs of $g[m]$ and $h[m]$:

$$X[r] = \underbrace{\sum_{m=0,1,2,\dots}^{K/2-1} g[m]e^{-j(2\pi mr/(K/2))}}_{G[r]} + e^{-j(2\pi r/K)} \underbrace{\sum_{m=0,1,2,\dots}^{K/2-1} h[m]e^{-j(2\pi mr/(K/2))}}_{H[r]} \quad (12.33)$$

or

$$X[r] = G[r] + W_K^r H[r], \quad (12.34a)$$

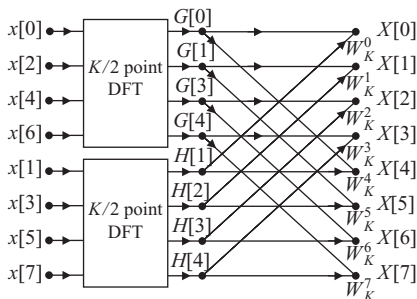
where W_K is defined as $\exp(-j2\pi/N)$ and is referred to as the twiddle factor. The $(K/2)$ -point DFTs $G[r]$ and $H[r]$ are defined as follows:

$$G[r] = \sum_{m=0,1,2,\dots}^{K/2-1} g[m]e^{-j(2\pi mr/(K/2))} \quad \text{and} \quad H[r] = \sum_{m=0,1,2,\dots}^{K/2-1} h[m]e^{-j(2\pi mr/(K/2))}. \quad (12.34b)$$

Equation (12.34b) implies that $G[r]$ represents the $(K/2)$ -point DFT coefficients of $g[k]$, the even-numbered samples of $x[k]$. Similarly, $H[r]$ represents the $(K/2)$ -point DFT coefficients of $h[k]$, the odd-numbered samples of $x[k]$. Equations (12.34) prove Proposition 12.6.1.

Based on Eqs (12.34), the procedure for determining the K -point DFT can be summarized by the following steps.

Fig. 12.10. Flow graph of a K -point DFT using two $(K/2)$ -point DFTs for $K = 8$.



- (1) Determine the $(K/2)$ -point DFT $G[r]$ for $0 \leq r \leq (K/2 - 1)$ of the even-numbered samples of $x[k]$.
- (2) Determine the $(K/2)$ -point DFT $H[r]$ for $0 \leq r \leq (K/2 - 1)$ of the odd-numbered samples of $x[k]$.
- (3) The K -point DFT coefficients $X[r]$ for $0 \leq r \leq (K - 1)$ of $x[k]$ are obtained by combining the $K/2$ DFT coefficients $G[r]$ and $H[r]$ using Eq. (12.34a). Although the index r varies from zero to $K - 1$, we only compute $G[r]$ and $H[r]$ over the range $0 \leq r \leq (K/2 - 1)$. Any outside value can be determined by exploiting the periodicity properties of $G[r]$ and $H[r]$, which state that

$$G[r] = G[r + K/2] \quad \text{and} \quad H[r] = H[r + K/2].$$

Figure 12.10 illustrates the flow graph for the above procedure for $K = 8$ -point DFT. In comparison with the direct computation of DFT using Eq. (12.30), Fig. 12.10 computes two $(K/2)$ -point DFTs along with K complex additions and K complex multiplications. Consequently, $(K/2)^2 + K$ complex additions and $(K/2)^2 + K$ complex multiplications are required with the revised approach. For $K > 2$, it is easy to verify that $(K/2)^2 + K < K^2$; therefore, the revised approach provides considerable savings over the direct approach.

Assuming that K is a power of 2, Proposition 12.6.1 can be applied on Eq. (12.34b) to compute the $(K/2)$ -point DFTs $G[r]$ and $H[r]$ as follows:

$$G[r] = \underbrace{\sum_{\ell=0,1,2,\dots}^{K/4-1} g[2\ell]e^{-j(2\pi\ell r/(K/4))}}_{G'[r]} + W_{K/2}^r \underbrace{\sum_{\ell=0,1,2,\dots}^{K/4-1} g[2\ell + 1]e^{-j(2\pi\ell r/(K/4))}}_{G''[r]} \tag{12.35}$$

and

$$H[r] = \underbrace{\sum_{\ell=0,1,2,\dots}^{K/4-1} h[2\ell]e^{-j(2\pi\ell r/(K/4))}}_{H'[r]} + W_{K/2}^r \underbrace{\sum_{\ell=0,1,2,\dots}^{K/4-1} h[2\ell + 1]e^{-j(2\pi\ell r/(K/4))}}_{H''[r]} \tag{12.36}$$

Fig. 12.11. Flow graphs of $(K/2)$ -point DFTs using $(K/4)$ -point DFTs. (a) $G[r]$; (b) $H[r]$.

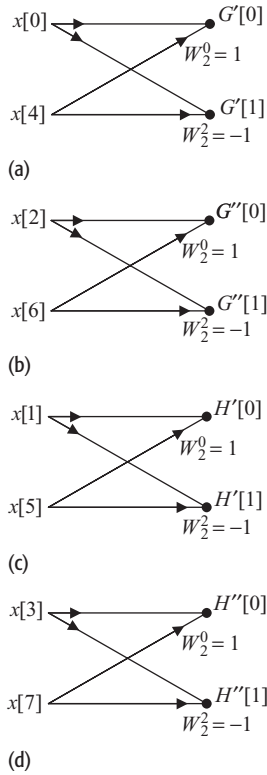
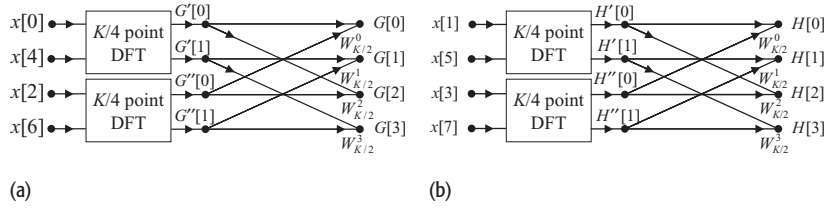


Fig. 12.12. Flow graphs of 2-point DFTs required for Fig. 12.11. (a) Top 2-point DFT $G'[0]$ and $G'[1]$ for Fig. 12.11(a). (b) Bottom 2-point DFT $G''[0]$ and $G''[1]$ for Fig. 12.11(a). (c) Top 2-point DFT $H'[0]$ and $H'[1]$ for Fig. 12.11(b). (d) Bottom 2-point DFT $H''[0]$ and $H''[1]$ for Fig. 12.11(b).



Equation (12.35) expresses the $(K/2)$ -point DFT $G[r]$ in terms of two $(K/4)$ -point DFTs of the even- and odd-numbered samples of $g[k]$. Figure 12.11(a) illustrates the flow graph for obtaining $G[r]$ using Eq. (12.35). Similarly, Eq. (12.36) expresses the $(K/2)$ -point DFT $H[r]$ in terms of two $(K/4)$ -point DFTs of the even- and odd-numbered samples of $h[k]$, which can be implemented using the flow graph shown in Fig. 12.11(b). If K is a power of 2, then the above process can be continued until we are left with a 2-point DFT. For the aforementioned example with $K = 8$, the $(K/4)$ -point DFTs in Fig. 12.11 can be implemented directly using 2-point DFTs. Using the definition of the DFT, the top left 2-point DFTs $G'[0]$ and $G'[1]$, for example, in Fig. 12.11(a) are expressed as follows:

$$G'[0] = x[0] e^{-j2\pi\ell r/2} \Big|_{\ell=0, r=0} + x[4] e^{-j2\pi\ell r/2} \Big|_{\ell=1, r=0} = x[0] + x[4] \quad (12.37)$$

and

$$G'[1] = x[0] e^{-j2\pi\ell r/2} \Big|_{\ell=0, r=1} + x[4] e^{-j2\pi\ell r/2} \Big|_{\ell=1, r=1} = x[0] - x[4]. \quad (12.38)$$

The flow graphs for Eqs (12.37) and (12.38) are shown in Fig. 12.12(a). By following this procedure, the flow diagrams for the remaining 2-point DFTs required in Fig. 12.11 are similarly derived and are shown in Figs 12.12(b)–(d).

Combining the individual flow graphs shown in Figs 12.10, 12.11, and 12.12, it is straightforward to derive the overall flow graph for the 8-point DFT, which is shown in Fig. 12.13; in this flow diagram, we have further reduced the number of operations for an 8-point DFT by noting that

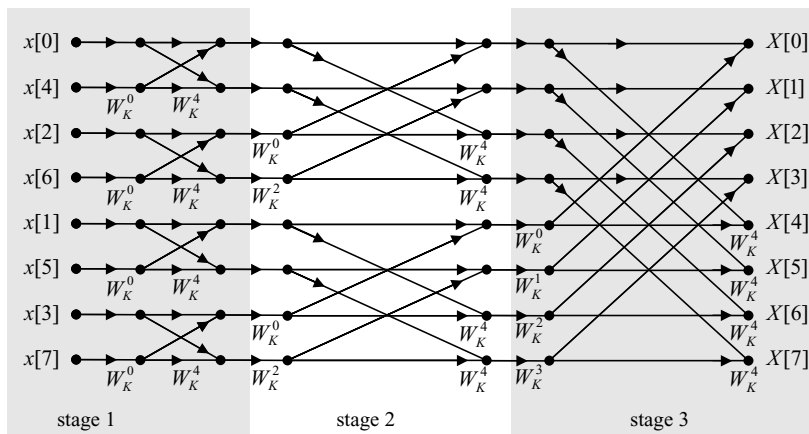
$$W_{K/2}^r = e^{-j2\pi r/(K/2)} = e^{-j4\pi r/K} = W_K^{2r},$$

and by placing the common terms between the twiddle multipliers of the two branches, which are originating from the same node, before the source node.

12.6.1 Computational complexity

To derive the computational complexity of the decimation-in-time algorithm, we generalize the results obtained in Fig. 12.13, where K is set to 8. We observe that Fig. 12.13 consists of $\log_2 K = 3$ stages and that each stage requires $K = 8$ complex multiplications and $K = 8$ complex additions. Therefore, the

Fig. 12.13. Decimation-in-time implementation of an 8-point DFT.



decimation-in-time FFT implementation for a K -point DFT requires a total of $K \log_2 K$ complex multiplications and $K \log_2 K$ complex additions.

Further reduction in the complexity of the decimation-in-time FFT implementation is obtained by observing that

$$W_K^0 = 1 \quad \text{and} \quad W_K^{K/4} = -1. \tag{12.39}$$

Multiplication by a factor of 1 can be ignored, while multiplication with -1 can be performed by a simple flip of the sign bit. Since each stage in Fig. 12.13 contains half such multiplications, the number of complex multiplications can be further reduced to $0.5K \log_2 K$ complex multiplications if all trivial multiplications of the types included in Eq. (12.39) are ignored. However, the number of complex additions stays the same at $K \log_2 K$.

Table 12.4 compares the number of computations for the direct implementation of Eq. (12.30) and the FFT implementation. The results are obtained by assuming that each complex multiplication requires four scalar multiplications and two scalar additions, while each complex addition requires two scalar additions. Since the direct implementation requires K^2 complex multiplications and K^2 complex additions, the number of scalar operations for the direct implementation is given by $8K^2$ flops. The number of scalar operations for the FFT implementation is $5K \log_2 K$ flops. For large values of K , say 8192, Table 12.4 illustrates a speed-up by up to a factor of 1000 with the FFT implementation. For real-valued sequences, the number of flops can be further reduced by exploiting the symmetry properties of the DFT.

12.6.2 Reordering of the input sequence

In Fig. 12.13, we observe that the input sequence $x[k]$ with length K has been arranged in an order that is considerably different from the natural order of

Table 12.4. Complexity of DFT calculation (in flops) with FFT and direct implementations

K	Number of flops		Increase in Speed
	FFT ($5K \log_2 K$)	direct ($8K^2$)	
32	800	8192	10.2
256	10 240	524 288	51.2
1024	51 200	8 388 608	163.8
8192	532 480	536 870 912	1 008.2

Table 12.5. Data reordering in radix-2 decimation-in-time FFT implementation

Original order, $x[k]$	Binary representation $x[b_2b_1b_0]$	Bit-reversed representation	
		binary $x[b_0b_1b_2]$	decimal $x_{re}[k]$
$x[0]$	$x[000]$	$x[000]$	$x[0]$
$x[1]$	$x[001]$	$x[100]$	$x[4]$
$x[2]$	$x[010]$	$x[010]$	$x[2]$
$x[3]$	$x[011]$	$x[110]$	$x[6]$
$x[4]$	$x[100]$	$x[001]$	$x[1]$
$x[5]$	$x[101]$	$x[101]$	$x[5]$
$x[6]$	$x[110]$	$x[011]$	$x[3]$
$x[7]$	$x[111]$	$x[111]$	$x[7]$

occurrence. This arrangement is referred to as the bit-reversed order and is obtained by expressing the index k in terms of $\log_2 K$ bits and then reversing the order of bits such that the most significant bit becomes the least significant bit, and vice versa. For $K = 8$, the reordering of the input sequence is illustrated in Table 12.5.

The function `myfft`, available in the accompanying CD, implements the radix-2 decimation-in-time FFT algorithm. Direct computation of the DFT coefficients using Eq. (12.16) is also implemented and provided as a second function, `mydft`. The reader should confirm that the two functions compute the same result, with the exception that the implementation of `myfft` is computationally efficient

As mentioned earlier, MATLAB also provides a built-in function `fft` to compute the DFT of a sequence. Depending on the length of the sequence, the `fft` function chooses the most efficient algorithm to compute the DFT. For example, when the length of the sequence is a power of 2, it uses the radix-2

algorithm. On the other hand, if the length is a prime number that cannot be factorized, it uses the direct method based on Eq. (12.16).

12.7 Summary

This chapter introduces the discrete Fourier transform (DFT) for time-limited sequences as an extension of the DTFT where the DTFT frequency Ω is discretized to a finite set of values $\Omega = 2\pi r/M$, for $0 \leq r \leq (M - 1)$. The M -point DFT pair for a causal, aperiodic sequence $x[k]$ of length N is defined as follows:

$$\text{DFT synthesis equation } x[k] = \frac{1}{M} \sum_{r=0}^{M-1} X[r] e^{j(2\pi kr/M)} \quad \text{for } 0 \leq k \leq (N - 1);$$

$$\text{DFT analysis equation } X[r] = \sum_{k=0}^{N-1} x[k] e^{-j(2\pi kr/M)} \quad \text{for } 0 \leq r \leq (M - 1).$$

For $M = N$, Section 12.2 implements the synthesis and analysis equations of the DFT in the matrix-vector format as follows:

$$\text{DFT synthesis equation } x = FX;$$

$$\text{DFT analysis equation } X = F^{-1}x,$$

where F is defined as the DFT matrix given by

$$F = \begin{bmatrix} 1 & 1 & 1 & \cdots & 1 \\ 1 & e^{-j(2\pi/N)} & e^{-j(4\pi/N)} & \cdots & e^{-j(2(N-1)\pi/N)} \\ 1 & e^{-j(4\pi/N)} & e^{-j(8\pi/N)} & \cdots & e^{-j(4(N-1)\pi/N)} \\ \vdots & \vdots & \vdots & \ddots & \vdots \\ 1 & e^{-j(2(N-1)\pi/N)} & e^{-j(4(N-1)\pi/N)} & \cdots & e^{-j(2(N-1)(N-1)\pi/N)} \end{bmatrix}.$$

The columns (or equivalently the rows) of the DFT matrix define the basis functions for the DFT.

Section 12.3 used the M -point DFT $X[r]$ to estimate the CTFT spectrum $X(\omega)$ of an aperiodic signal $x(t)$ using the following relationship:

$$X(\omega_r) \approx \frac{MT_1}{N} X_2[r],$$

where T_1 is the sampling interval used to discretize $x(t)$, ω_r are the CTFT frequencies that are given by $2\pi r/(M \times T_1)$ for $-0.5(M-1) \leq r \leq 0.5(M-1)$, and N is the number of samples obtained from the CT signal. Similarly, the DFT $X[r]$ can be used to determine the DTFT $X(\Omega)$ of a time-limited sequence $x[k]$ of length N as

$$X_2(\Omega_r) = \frac{N}{M} X_2[r]$$

at discrete frequencies $\Omega_r = 2\pi r/M$, for $0 \leq r \leq (M - 1)$.

Section 12.4 covered the following properties of the DFT.

- (1) The periodicity property states that the M -point DFT of a sequence is periodic with period M .
- (2) The orthogonality property states that the basis functions of the DFTs are orthogonal to each other.
- (3) The linearity property states that the overall DFT of a linear combination of DT sequences is given by the same linear combination of the individual DFTs.
- (4) The Hermitian symmetry property states that the DFT of a real-valued sequence is Hermitian. In other words, the real component of the DFT of a real-valued sequence is even, while the imaginary component is odd.
- (5) The time-shifting property states that shifting a sequence in the time domain towards the right-hand side by an integer constant m is equivalent to multiplying the DFT of the original sequence by a complex exponential given by $\exp(-j2\pi m/M)$. Similarly, shifting towards the left-hand side by an integer m is equivalent to multiplying the DTFT of the original sequence by a complex exponential given by $\exp(j2\pi m/M)$.
- (6) The time-convolution property states that the periodic convolution of two DT sequences is equivalent to the multiplication of the individual DFTs of the two sequences in the frequency domain.
- (7) Parseval's theorem states that the energy of a DT sequence is preserved in the DFT domain.

Section 12.5 used the convolution property to derive alternative procedures for computing the convolution sum. These procedures are computationally optimal and use fast Fourier transform (FFT) implementations for the DFT to provide considerable savings over the direct implementation of the convolution sum.

Section 12.6 covers the decimation-in-time FFT implementation of the DFT. In deriving the FFT algorithm, we assume that the length N of the sequence equals the number M of samples in the DFT, i.e. $N = M = K$. We showed that if K is a power of 2, then the FFT implementations have a computational complexity of $O(K \log_2 K)$.

Problems

12.1 Determine analytically the DFT of the following time sequences, with length $0 \leq k \leq (N - 1)$:

$$(i) \ x[k] = \begin{cases} 1 & k = 0, 3 \\ 0 & k = 1, 2 \end{cases} \text{ with length } N = 4;$$

12 Discrete Fourier transform

(ii) $x[k] = \begin{cases} 1 & k \text{ even} \\ -1 & k \text{ odd} \end{cases}$ with length $N = 8$;

(iii) $x[k] = 0.6^k$ with length $N = 8$;

(iv) $x[k] = u[k] - u[k - 8]$ with length $N = 8$;

(v) $x[k] = \cos(\omega_0 k)$ with $\omega_0 \neq 2\pi r/N$.

12.2 Determine the DFT of the time-limited sequences specified in Examples 12.1(i)–(iv) using the matrix-vector approach.

12.3 Determine the time-limited sequence, with length $0 \leq k \leq (N-1)$, corresponding to the following DFTs $X[r]$, which are defined for the DFT index $0 \leq r \leq (N-1)$:

(i) $X[r] = [1 + j4, -2 - j3, -2 + j3, 1 - j4]$ with $N = 4$;

(ii) $X[r] = [1, 0, 0, 1]$ with $N = 4$;

(iii) $X[r] = \exp -j(2\pi k_0 r/N)$, where k_0 is a constant;

(iv) $X[r] = \begin{cases} 0.5N & r = k_0, N - k_0 \\ 0 & \text{elsewhere} \end{cases}$ where k_0 is a constant;

(v) $X[r] = \begin{cases} k_0 & r = 0 \\ e^{-j(\pi r(N-1)/N)} \frac{\sin(\pi r k_0/N)}{\sin(\pi r/N)} & r \neq 0 \end{cases}$ where k_0 is a constant;

(vi) $X[r] = \left(\frac{r}{N}\right)$ for $0 \leq r \leq (N-1)$.

12.4 In Problem 11.1, we determined the DTFT representation for each of the following DT periodic sequences using the DTFS. Using MATLAB, compute the DTFT representation based on the FFT algorithm. Plot the frequency characteristics and compare the computed results with the analytical results derived in Chapter 11.

(i) $x[k] = \cos(10\pi k/3) \cos(2\pi k/5)$;

(ii) $x[k] = |\cos(2\pi k/3)|$;

(iii) $x[k] = k$ for $0 \leq k \leq 5$ and $x[k + 6] = x[k]$;

(iv) $x[k] = \sum_{m=-\infty}^{\infty} \delta(k - 5m)$;

(v) $x[k] = \begin{cases} 1 & 0 \leq k \leq 2 \\ 0.5 & 3 \leq k \leq 5 \\ 0 & 6 \leq k \leq 8 \end{cases}$ and $x[k + 9] = x[k]$;

(vi) $x[k] = 2 \exp\left(j\frac{5\pi}{3}k + \frac{\pi}{4}\right)$;

(vii) $x[k] = 3 \sin\left(\frac{2\pi}{7}k + \frac{\pi}{4}\right)$.

12.5 (a) Using the FFT algorithm in MATLAB, determine the DTFT representation for the following sequences. Plot the magnitude and phase spectra in each case.

(i) $x[k] = k3^{-|k|}$ for all k ;

(ii) $x[k] = \alpha^k \cos(\omega_0 k)u[k]$, $|\alpha| < 1$;

(iii) $x[k] = -5$ for all k ;

(iv) $x[k] = \sum_{m=-\infty}^{\infty} \delta(k - 5m - 3)$;

(v) $x[k] = \alpha^k \sin(\omega_0 k + \phi)u[k]$, $|\alpha| < 1$;

(vi) $x[k] = \frac{\sin(\pi k/5) \sin(\pi k/7)}{\pi^2 k^2}$.

(b) Compare the obtained results with the analytical results derived in Problem 11.4(a).

12.6 Using the FFT algorithm in MATLAB, determine the CTFT representation for each of the following CT functions. Plot the frequency characteristics and compare the results with the analytical results presented in Table 5.1.

(i) $x(t) = e^{-2t}u(t)$;

(ii) $x(t) = e^{-4|t|}$;

(iii) $x(t) = t^4 e^{-4t}u(t)$;

(iv) $x(t) = e^{-4t} \cos(10\pi t)u(t)$;

(v) $x(t) = e^{-t^2/2}$;

12.7 Prove the Hermitian property for the DFT.

12.8 Prove the time-shifting property for the DFT.

12.9 Prove the periodic-convolution property for the DFT.

12.10 Prove Parseval's relationship for the DFT.

12.11 Without explicitly determining the DFT $X[r]$ of the time-limited sequence

$$x[k] = [6 \ 8 \ -5 \ 4 \ 16 \ 22 \ 7 \ 8 \ 9 \ 44 \ 2],$$

compute the following functions of the DFT $X[r]$:

(i) $X[0]$; (iv) $\sum_{r=0}^{10} X[r]$;
 (ii) $X[10]$;
 (iii) $X[6]$; (v) $\sum_{r=0}^{10} |X[r]|^2$.

12 Discrete Fourier transform

12.12 Without explicitly determining the the time-limited sequence $x[k]$ for the following DFT:

$$X[r] = [12 \ 8 + j4 \ -5 \ 4 + j1 \ 16 \ 16 \ 4 - j1 \ -5 \ 8 - j4],$$

compute the following functions of the DFT $X[r]$:

$$\begin{aligned} \text{(i)} \quad & x[0]; & \text{(iv)} \quad & \sum_{r=0}^9 x[k]; \\ \text{(ii)} \quad & x[9]; & & \\ \text{(iii)} \quad & x[6]; & \text{(v)} \quad & \sum_{r=0}^9 |x[k]|^2; \end{aligned}$$

12.13 Given the DFT pair

$$x[k] \xleftrightarrow{\text{DFT}} X[r],$$

for a sequence of length N , express the DFT of the following sequences as a function of $X[r]$:

$$\begin{aligned} \text{(i)} \quad & y[k] = x[2k]; \\ \text{(ii)} \quad & y[k] = \begin{cases} x[0.5k] & k \text{ even} \\ 0 & \text{elsewhere;} \end{cases} \\ \text{(iii)} \quad & y[k] = x[N - k - 1] \quad \text{for } 0 \leq k \leq (N - 1); \\ \text{(iv)} \quad & y[k] = \begin{cases} x[k] & 0 \leq k \leq N - 1 \\ 0 & N \leq k \leq 2N - 1; \end{cases} \\ \text{(v)} \quad & y[k] = (x[k] - x[k - 2])e^{j(10\pi k/N)}. \end{aligned}$$

12.14 Compute the linear convolution of the following pair of time-limited sequences using the DFT-based approach. Be careful with the time indices of the result of the linear convolution.

$$\begin{aligned} \text{(i)} \quad & x_1[k] = \begin{cases} k & 0 \leq k \leq 3 \\ 0 & \text{otherwise} \end{cases} \quad \text{and} \quad x_2[k] = \begin{cases} 2 & -1 \leq k \leq 2 \\ 0 & \text{otherwise;} \end{cases} \\ \text{(ii)} \quad & x_1[k] = k \text{ for } 0 \leq k \leq 3 \quad \text{and} \quad x_2[k] = \begin{cases} 5 & k = 0, 1 \\ 0 & \text{otherwise;} \end{cases} \\ \text{(iii)} \quad & x_1[k] = \begin{cases} 2 & 0 \leq k \leq 2 \\ 0 & \text{otherwise} \end{cases} \quad \text{and} \quad x_2[k] = \begin{cases} k + 1 & 0 \leq k \leq 4 \\ 0 & \text{otherwise;} \end{cases} \\ \text{(iv)} \quad & x_1[k] = \begin{cases} -1 & k = -1 \\ 1 & k = 0 \\ 2 & k = 1 \\ 0 & \text{otherwise} \end{cases} \quad \text{and} \quad x_2[k] = \begin{cases} 3 & k = -1, 2 \\ 1 & k = 0 \\ -2 & k = 1, 3 \\ 0 & \text{otherwise;} \end{cases} \\ \text{(v)} \quad & x_1[k] = \begin{cases} |k| & |k| \leq 2 \\ 0 & \text{otherwise} \end{cases} \quad \text{and} \quad x_2[k] = \begin{cases} 2^{-k} & 0 \leq k \leq 3 \\ 0 & \text{otherwise.} \end{cases} \end{aligned}$$

12.15 Draw the flow graph for a 6-point DFT by subdividing into three 2-point DFTs that can be combined to compute $X[r]$. Repeat for the

subdivision of two 3-point DFTs. Which one provides more computational savings?

- 12.16** Draw a flow graph for a 10-point decimation-in-time FFT algorithm using two DFTs of size 5 in the first stage of the flow graph and five DFTs of size 2 in the second stage. Compare the computational complexity of the algorithm with the direct approach based on the definition.
- 12.17** Assume that $K = 3^3$. Draw the flow graph for a K -point decimation-in-time FFT algorithm consisting of three stages by using radix-3 as the basic building block. Compare the computational complexity of the algorithm with the direct approach based on the definition.